NATIONAL ADVISORY COMMITTEE FOR AERONAUTICS

TECHNICAL NOTE

No. 1586

INVESTIGATION OF EFFECTIVENESS OF AIR-HEATING A HOLLOW STEEL PROPELLER FOR PROTECTION AGAINST ICING

I - UNPARTITIONED BLADES

By Donald R. Mulholland and Porter J. Perkins

Flight Propulsion Research Laboratory
Cleveland, Ohio

Washington
May 1948

NATIONAL ADVISORY COMMITTEE FOR AERONAUTICS

TECHNICAL NOTE NO. 1586

INVESTIGATION OF EFFECTIVENESS OF AIR-HEATING A HOLLOW STEEL PROPELLER FOR PROTECTION AGAINST ICING

I - UNPARTITIONED BLADES

By Donald R. Mulholland and Porter J. Perkins

SUMMARY

An investigation to determine the effectiveness of icing protection afforded by air-heating hollow steel unpartitioned propeller blades has been conducted in the NACA Cleveland icing research tunnel. The propeller used was a production model modified with blade shank and tip openings to permit internal passage of heated air. Blade-surface and heated-air temperatures were obtained and photographic observations of ice formations were made with variations in icing intensity and heating rate to the blades.

For the conditions of icing to which the propeller was subjected, it was found that adequate ice protection was afforded with a heating rate of 40,000 Btu per hour per blade. With less than 40,000 Btu per hour per blade, ice protection failed because of significant ice accretions on the leading edge. The chordwise distribution of heat was unsatisfactory with most of the available heat dissipated well back of the leading edge on both the thrust and camber faces instead of at the leading edge where it was most needed. A low utilization of available heat for icing protection is indicated by a heat-exchanger effectiveness of approximately 47 percent.

INTRODUCTION

As the demand for all-weather protection on aircraft for unimpaired and continuous commercial and military service developed, the detrimental effects of propeller icing on airplane performance became increasingly important. Early attempts toward some means of propeller icing protection centered around the use of anti-icing pastes and slinger-ring arrangements for distributing anti-icing fluids on the propeller-blade surfaces. More recently, electric de-icing systems using external rubber-clad electric heating elements have been employed with a comparative high degree of success (reference 1). Attempts have also been made to use internal electric heaters, which inherently eliminate the possibility of erosion damage and preserve the aerodynamic performance of the blade surface.

A system has been recently devised whereby the propeller blades are heated by passage of a hot gas through the cavity of hollow steel blades. Previous evaluation of the thermal performance using the hot-air means of propeller heating is reported in reference 2, and flight icing observations using such propeller heating have been made by the Curtiss Wright Corporation.

An investigation was conducted in the icing research tunnel of the NACA Cleveland laboratory using a production-model propeller the blades of which were modified with shank and tip openings for the internal passage of heated air. The tip orifices differed slightly from those on the blades used in the two previously mentioned investigations of air-heated propellers. Data were taken to determine the effectiveness of the blade-heating system, blade-surface temperatures, and heat requirements, as well as to obtain observations of the icing protection afforded by the heating system.

The complete research program involved investigation of air-heating (1) fully hollow unpartitioned propeller blades, (2) propeller blades partitioned to confine the air flow to the forward one-half of the blade cavity, and (3) propeller blades partitioned to confine the air flow to the forward one-fourth of the blade cavity. Only the unpartitioned-blade configuration is considered herein. Blade-surface temperatures were measured by means of ribbon-type thermocouples faired into a smooth plastic coating. Such a system reduced the disturbance of the air flow behind successive thermocouples to a minimum.

SYMBOLS

The following symbols are used in this report:

b blade chord, feet

c_p specific heat of air at constant pressure, 0.24 Btu per pound per °F

d propeller diameter, 10 feet, 2 inches

g acceleration of gravity, 32.2 feet per second per second

h blade thickness, feet

J mechanical equivalent of heat, 778 foot pounds per Btu

N propeller speed, rpm

Q heating rate, Btu per hour per blade

t_a indicated tunnel air temperature, °F

t_c heated-air temperature at blade shank collar, °F

t_s blade-surface temperature, °F

t_t heated-air temperature at blade tip, °F

V_a tunnel air velocity, feet per second

V_t propeller tip velocity, feet per second

β blade angle, degrees

η blade heat-exchanger effectiveness, percent

APPARATUS

Propeller installation. - The icing research tunnel in which the propeller icing investigation was conducted is a return-type tunnel of rectangular cross section. Full-scale operating conditions were achieved by mounting a propeller in the main diffuser of the tunnel at a point where the tunnel dimensions are approximately 15 by 12 feet (fig. 1) and maximum air velocities are approximately 200 feet per second. A modified airplane fuselage containing a liquid-cooled engine was installed in the tunnel to support and drive the propeller. A four-blade production-model hollow steel propeller of 10-foot 2-inch diameter, modified with shank and tip openings to permit the internal flow of heated air, was used for the icing investigation. The propeller-blade characteristics are presented in figure 2.

The instrumentation space requirements for temperature measurements necessitated the removal of the electric pitch-change motor assembly and the use of a special pitch gear that locked the propeller blades at any desired pitch.

Spray system. - Icing conditions were established in the tunnel when water was admitted to the spray system, which consists of a ring of 46 air-atomizing spray nozzles. The nozzles discharge water perpendicularly into the air stream immediately upstream of the tunnel contraction at a point 117 feet ahead of the propeller.

Propeller-blade heating system. - Heated air was supplied to the propeller from electric heaters outside the tunnel. Automatically controlled dampers, which mixed heated and unheated air, maintained the desired temperature. As shown in figure 3, the de-icing air entered tangentially into a stationary scroll-type manifold provided with several outlets to the space between the manifold and the revolving spinner. Four holes in the spinner rear bulkhead admitted air into collars, which surround each blade shank, from which the air entered the blade to be discharged through a tip orifice. Construction details and photographs of the shank inlets and discharge orifice are shown in figure 4.

The blade was so designed that the tip-orifice area determined the maximum flow of air through the blades. Propeller-efficiency losses associated with air flow through a tip orifice on similar propeller blades are reported in reference 3 to be a maximum of 3 percent. It was computed that the power required to pump 425 pounds of air per hour per blade at a propeller speed of 1050 rpm amounted to about 2 horsepower per blade.

A segmented graphite seal confined in a groove in the outer edge of the stationary manifold reduced the air leakage between the stationary and rotating members. The graphite segments were permitted to rotate in contact with the overhanging edge of the spinner bulkhead. (See fig. 3) Sliding contact carbon rings in each blade-shank collar provided air seals at the blade shanks and permitted pitch adjustment.

The primary source of air entered the electric heaters outside the tunnel at atmospheric pressure. Losses in the heater and ducting system, in combination with the pumping action of the revolving blade, reduced the pressure in the manifold to some value below the tunnel pressure. The pumping action of the blade and the pressure losses at the blade shank and the blade tip were of such magnitude that the air was discharged from the blade at tunnel pressure. Because the tunnel pressure exceeded the manifold pressure, air leaked into the system from the tunnel past the graphite seals. This secondary source of air then became a part of the blade air flow.

INSTRUMENTATION

The instrumentation used during the investigation provided for measurement of tunnel and propeller operating conditions, propeller heated-air temperatures and mass flow, and blade-surface temperatures.

Stroboscopic flash lamps, which were mounted in the tunnel wall and synchronized with the propeller tachometer, made it possible to observe the propeller blades during the icing period and to obtain stroboscopic pictures of the blades during icing supplementing still pictures of residual icing.

Tunnel. - Free-air temperature was determined through use of four bullet-nosed shielded-type thermocouples constructed to prevent ice formation on the junction. Two of these thermocouples were placed 12 feet upstream and two were placed 25 feet downstream of the propeller plane; the four readings obtained were averaged.

Average free-stream liquid-water content, droplet size, and air velocity were determined from tunnel calibrations made prior to the propeller investigation. Reference velocity measurements were made with electrically heated coaxial pitot static and total-head tubes mounted 12 feet ahead of the propeller.

Blade-heating system. - The rate of flow of heated air to the propeller was measured by means of a flat plate orifice installed in the air duct leading from the electric heaters. Temperatures of the hot air were measured at the orifice, at several points in the stationary manifold behind the spinner, at the blade-shank inlets, and at the tip orifices.

The leakage past the graphite seals at the rear of the spinner and around the blade shanks (fig. 3) was found to be sufficient to require a correction in the heated-air flow. This leakage was calibrated against the differential pressure across the segmented spinner seal by temporarily blocking off the air flow to the blades at the shank inlets and forcing hot air into the manifold and out past the seals with a blower attached at the inlet to the electric heaters. The calibration was conducted at the propeller speeds used during icing but no leakage change with propeller-speed variation was noted. The calibration curve used for correction of the air flow during the icing work is given in figure 5. The lower segments of this curve represent the calibration data; however, inasmuch as the manifold pressure was less than tunnel pressure and air leaked in during normal operation, a mirror-image curve for the same leakage range was constructed above the original curve and used to correct the propeller heated-air flow. During calibration, a heated-air temperature of 400° F was used in the manifold to determine the leakage out; therefore, the mirror-image curve was corrected for an average tunnel-air temperature of 15° F.

Blade-surface temperatures. - Chordwise blade-surface temperature measurements were obtained from thermocouples placed at 40- and 70-percent radii on two of the four blades. Locations of these thermocouples are shown in figure 6.

Iron and constantan wire ribbons of approximately 0.0015-inch thickness were spot-welded to the blade at the point of temperature measurement, as shown in figure 7. This method of attachment provides a sound thermocouple junction and sufficient mass at the junction to prevent significant conduction along the thermocouple leads. The ribbon leads extended to the trailing edge and were insulated from the blade metal and faired to a smooth final surface with thin layers of plastic cement. At the trailing edge, the wire in round cotton-insulated form was cemented to the blade and extended to the hub.

This type of installation for temperature measurements on rotating members was satisfactory except for the leading-edge thermocouples, which were subjected to extreme abrasion by water. Most of these thermocouples failed before completion of the program.

The system for measuring the heated-air and blade-surface temperatures was designed to record automatically all blade and manifold temperatures in $1\frac{1}{2}$ minutes. Accumulative errors in the measuring circuit gave accuracies of the recorded temperatures to about 2° F for values below 100° F and about 3° F for values above 100° F.

CONDITIONS AND PROCEDURE

Tunnel conditions. - The propeller was subjected to icing conditions at ambient-air temperatures from -9° to 19° F. The maximum tunnel-air velocity at the propeller was 200 feet per second measured at 75-percent propeller radius. Under nonicing conditions, the radial velocity distribution shown in figure 8 provided higher air velocities toward the center of rotation and slightly lower velocities near the blade tips. The velocity at 75-percent radius was chosen as the nominal reference velocity for propeller work. With constant maximum tunnel-fan speed, icing of the tunnel sufficiently reduced the mass flow to cause significant reductions in velocity at the propeller. This condition resulted in further reductions of velocity on the outer portions of the propeller radius with less significant changes in velocity near the center of rotation. (See fig. 8.)

The liquid-water concentration, determined from a previous calibration, varied with air temperature (fig. 9) and ranged from approximately 0.1 to 0.9 gram per cubic meter for air temperatures from 3° to 19° F. The effective droplet diameter based on the volume maximum was found in a preliminary investigation to be approximately 55 microns over the entire range of icing temperatures. This value is known to be large compared to droplet diameters usually encountered in flight. The collection efficiency of propeller blades with small leading-edge radii, however, is practically independent of droplet size, decreasing only slightly with smaller droplet diameters. Very small droplets would result in less chordwise extent of icing. The heating values required in this investigation are therefore considered to be conservative if very small droplet diameters are encountered. Further details of tunnel-icing and operating conditions pertaining to propeller icing research may be found in reference 1.

Range of propeller variables. - The propeller was operated at two blade angles, 28° and 35°, at which advance ratios $(60V_a/Nd)$ of 1.1 and 1.4, respectively, were established to approximate the advance ratio corresponding to peak efficiency. The low maximum available tunnel-air velocity, however, limited the propeller speeds to 1050 and 850 rpm for the respective blade angles.

The pumping action of the propeller, together with a boost pressure of 16 inches of water (produced by the pressure difference between the atmosphere and the tunnel) and the friction loss in the air heating system established the heated-air flow from 400 to 450 pounds per hour per blade at 1050 rpm and 350 to 400 pounds per hour per blade at 850 rpm.

Typical procedure. - Data were obtained during 10-minute periods of simulated icing conditions. Prior to each icing period, data were recorded for 2 minutes with all the operating conditions stablized and heated air flowing through the blades. Surface temperatures on one propeller blade were recorded continuously throughout the preicing and icing period. Following each icing condition, residual icing photographs were obtained, and the propeller and the tunnel were thoroughly cleaned of ice deposits by means of a steam spray.

RESULTS AND DISCUSSION

Blade-Heating System

The air-flow and thermal characteristics of the heating system were investigated to determine the effectiveness of the unpartitioned blade as a heat exchanger. The blade heat-exchanger effectiveness for a propeller speed of 1050 rpm with no sprays on in the tunnel is shown in figure 10 as a function of heating rate. The blade heat-exchanger effectiveness has been considered as the ratio of the heat dissipated by the blade to the total heating rate to the blade and was calculated by the following equation:

$$\eta = \frac{t_c - t_t}{t_c - t_a + \left(\frac{V_t^{\,2}}{2Jgc_p}\right)}$$

The heating rate represented by $(t_c - t_a)$ is augmented by the equivalent heating of the internal air by centrifugal compression. The values of effectiveness from approximately 41 to 49 percent, shown in figure 10, are not considered unreasonably low for the passage of air through a propeller blade. The heat-exchanger effectiveness would be increased with a reduction in air flow or an increase in cuff temperature. The rise in heat-exchanger effectiveness with increasing heating rate (fig. 10) results from the increase in cuff temperature at a constant air flow.

Observations of the blade-shank interior after operation showed considerable sooting by graphite dust worn from the air seals. Should such sooting persist throughout the interior of the blade, heat transfer would be reduced by the insulating qualities of the deposit and the heat-exchanger effectiveness would be adversely affected.

The heat transfer along the leading edge, the area most critical with respect to ice formation, suffers materially from the narrow passage afforded the air flow at this section. The restricted area for internal heat transfer arising from the small internal perimeter (compared to the external perimeter) contributes to reducing effectiveness of the air heating at the leading edge.

The rotational forces acting on the internal air flow during propeller operation probably create a high-pressure area near the trailing edge of the blade and develop pressure gradients chordwise across the blade with high velocities at the leading edge. This action would be most pronounced at the inboard sections of the blade because the cavity is more nearly circular. As the blade begins to flatten, the flow is believed to be concentrated near the center of the chord because of the narrow leading-edge passage; beyond approximately 55-percent radius, blade-surface temperatures indicate almost complete separation of the internal flow from the fore part of the blade. Thus little heating of the leading edge is provided on the outboard sections.

A detailed theoretical analysis of heat transfer on similar propeller blades that are heated by means of internal air flow is given in reference 4.

Blade-Surface Temperatures

The temperature data obtained from the thermocouples located on the blade surfaces are presented as the rise in temperature of the surface above the indicated tunnel-air temperature. This temperature rise is presented as a function of both the position on the blade surface and the heating rate to the blade. In the isometric representation (fig. 11), the blade-surface temperature rise is shown on the verticle axis. On the axis designating the location of the temperature measurement, the blade surface is laid out in plan form with the leading edge as the center and the distance over the thrust and camber faces extending along the axis on either side. The third axis indicates the heating rate to the blade. Each blade-surface temperature-rise contour represents data recorded in a single 1/2 minute of stabilized tunnel conditions and heating rate to the propeller.

Representative curves in figure 11 show blade-surface temperature distributions taken at the 40- and 70-percent radii under no-spray and icing conditions at a propeller speed of 1050 rpm. The data with no sprays were obtained during a 2-minute period prior to turning on the sprays in the tunnel. During this period, the tunnel conditions and propeller variables were held constant at previously stabilized values.

When conditions for icing prevail in the tunnel, the blade-surface temperatures vary with time, even when tunnel-air conditions and blade-heating rate are held constant, because of the formation and shedding of ice. The data shown in figure 11 are therefore true only for a given instant and need not be representative of average temperatures under icing conditions.

Plots for average temperatures, under both no-spray and icing conditions, are shown in figure 12. In developing the average curves, the relation of blade-surface temperature rise to heating rate was assumed to be independent of the tunnel-air temperature.

Accordingly, all readings for each thermocouple on the blade surface were plotted against heating rate. A linear relation was assumed between the two variables and a straight line was drawn as an average of the data for each thermocouple. From these plots, temperature-distribution curves were constructed for heating rates of 25,000, 30,000, 35,000, and 40,000 Btu per hour per blade.

These curves show the inefficient distribution of the applied heat to unpartitioned blades. For example, at 40-percent radius and a heating rate of 40,000 Btu per hour per blade (fig. 12(a)), the surface temperatures near 20-percent chord on the camber face just prior to turning on the sprays are over 35° F higher than those at the leading edge where the heat is most needed. Also, by increasing the heating rate from 25,000 to 40,000 Btu per hour per blade, the leading-edge temperature at the 70-percent station is raised only 7° F (fig. 12(b)). Such results show an extreme waste of heat creating excessively high surface temperatures back of the leading edge on both the thrust and camber faces.

The inflections in the distribution curves for the 40-percent radial station (fig. 12(a)) at about 20-percent chord on both thrust and camber faces indicate the possible transition from laminar to turbulant flow at this point. At high heating rates, this transition apparently disappears from the thrust face but remains on the camber face. The combination of greater chordwise heat conduction in the metal for higher temperature gradients and less turbulent flow over the thrust face could account for the more uniform distribution on the thrust face than on the camber face.

The effects of wetting the blade surface are most significant as shown by comparing the no-spray and icing conditions for the same heating rate to the blade (fig. 13). In an icing-spray cloud, the leading edge and the camber face at 40-percent radius are 15° to 30° F lower than for no-spray conditions.

The higher local velocities over the camber face as compared to the thrust face result in greater cooling of the surface, as shown in the temperature distribution at the 70-percent radial station (fig. 14). The difference between the temperatures on the thrust and camber faces was less at 40-percent radius than at 70-percent radius because the difference between the velocities on the two faces was not as great at the smaller radius. Change of blade angle and propeller speed have very little effect on the general temperature distribution for the range of propeller variables investigated. A change of propeller speed from 1050 to 850 rpm, however, resulting from a change of blade angle from 28 to 35 degrees for a given heating rate lowered the internal mass air flow and raised the heated-air temperature, consequently surface temperatures were higher. In addition, at the lower propeller speed the blade-surface temperature was increased because of the resultant reduced external convective cooling.

Icing Observations

Unheated condition. - Typical unheated propeller-blade ice formations, taken after 10-minute icing periods, are shown in the photograph of figure 15. Stroboscopic photographs taken during propeller operation are shown in figure 16. The photograph on the left of figure 16 is to be used as a key for the stroboscopic photographs of that figure as well as all subsequent stroboscopic photographs. It illustrates the blade positions when stroboscopic pictures were taken so that photographs of the blade in the up position show the thrust face and photographs in the down position show the camber face of the propeller blades.

At the higher tunnel-air temperatures, which were accompanied by relatively high liquid-water contents (fig. 9), very rough combination rime- and glaze-ice formations occurred as compared to smoother and harder rime icing that occurred at lower temperatures. A comparison of the two types of icing obtained at 16° and 10° F is shown in figure 15. The difference in the type of icing is especially evident on the airplane fuselage in the upper photographs.

Although high liquid-water contents existed at high air temperatures, the most bulky propeller ice formations occurred near 10° to 12° F (figs. 15(b) and 16). Much of the water available for propeller icing at higher temperatures did not freeze because of the higher blade temperatures, especially on the outer portions of the blades where kinetic heating was most effective. Under these conditions of temperature and liquid-water content, much of the ice formation occurred as runback. (See fig. 15(a).)

The camber face showed a greater tendency to ice under all conditions than did the thrust face. Very little icing occurred on the thrust face at the higher tunnel-air temperatures except as runback, which extended to approximately 70 percent of the radius over most of the thrust face. The camber-face ice formations were heaviest over the leading-edge region near the shanks, tapering toward the trailing edge and toward the blade tip. (See fig. 16.) Initial ice deposits on the extreme leading edge were invariably smooth and sharp, extending forward in some cases as much as 3/4 inch. The area of icing was not noticeably affected by propeller speed for the range of speeds employed.

With severe icing conditions (10° to 12° F), partial shedding usually occurred between 20 and 50 percent of the radius within the first 7 minutes of icing. Further operation resulted in erratic shedding and reformation leaving a jagged ice structure, as shown in figure 16. Higher tunnel-air temperatures lengthened the time before the first throw-off, and shedding was usually confined to the extreme leading-edge region. Back of the leading edge shedding became less apparent as the ambient-air temperature was increased above that at which severest icing occurred.

Heated condition. - Photographs of residual ice formation on the camber faces of propeller blades following a 10-minute icing period are shown in figure 17 for several heating rates and at several tunnel-air temperatures. Figure 18 shows, by means of stroboscopic photographs taken during propeller operation, progressive ice formation on heated blades as well as residual icing.

At propeller speeds of 1050 rpm using a blade angle of 28° (fig. 17), heating rates up to 40,000 Btu per honr per blade were obtained. Compared to electric heating, this heating rate corresponds to an average of approximately 8 watts per square inch over the entire blade area, or approximately 3.8 watts per square inch actually dissapated to the blade, considering the blade heat-exchanger effectiveness to be 47 percent. Under the most severe condition of icing at 10° F, a heating rate of 39,400 Btu per hour per blade resulted in practically complete icing prevention except for a very small formation at the leading edge near 60 percent of the radius on three of the four blades (fig. 17(d)); this icing is not considered sufficient to affect propeller operation. Lowering the heating rate to 26,000 Btu per hour per blade at 10° F resulted in less satisfactory icing protection at the leading edge, as shown in figure 17(c). The ice formation shown for this condition is not considered severe although it occurs over the critical working radius of the blade. Reference 5, which gives the results of simulated icing on propeller performance, indicates that disturbances attributed to relatively smooth simulated glaze icing at the leading edge caused a maximum loss in peak efficiency of 3 percent for level flight and also indicated that such a loss would be increased to as much as 15 percent during climb.

At the lowest tunnel-air temperature, (-2° F), a heating rate of 40,000 Btu per hour per blade provided complete protection for the conditions that prevailed in the tunnel (fig. 17(f)), although it is known that the condition of icing at that temperature was not severe because of the low liquid-water content. For this reason, the effect of such heating during severe low-temperature icing conditions was not demonstrated except through measurement of the surface temperatures shown in figure 12. Inasmuch as the surface temperatures were found to be appreciably below freezing, it was assumed that the maximum heat available using unpartitioned blades would be insufficient to afford protection near the leading edge if severe icing conditions were encountered at low tunnel-air temperatures.

The stroboscopic photographs shown in figure 18 illustrate the progressive effectiveness of the heating system compared with the unheated condition in figure 16. In each case, the propeller speed is 850 rpm during icing conditions at tunnel-air temperatures of 9° F and 11° F. With heating conditions insufficient for complete icing protection, early formation occurred on the leading edge from 20-percent radius to the extreme tip within the first 1/2 minute. (See fig. 18(a).) Usually this light formation would recede from the tip very quickly because of the erosion effect of the ice particles in the air stream. Remaining ice on the blade would then build up in thickness by an amount dependent upon the effectiveness of internal heating. The first throw-off usually occurred near 40-percent radius. Leading-edge ice formations did not extend more than 1 inch on the thrust face even with heating rates as low as 26,000 Btu per hour per blade, but did extend as much as 2 inches on the camber face. General observations indicated little effect of propeller speed on the area of icing although in specific instances less ice was apparent at 1050 rpm than at 850 rpm.

General Remarks

The effectiveness of increasing blade heating at tunnel-air temperatures from -9° to 19° F indicate that extremely large quantities of heat are necessary to prevent ice formations at the blade leading edge using unpartitioned blades in severe icing conditions. Most of the heat is dissipated from the blade surface well back of the leading edge, as indicated by the chordwise surface temperatures, so that much of the surface would be at an unnecessarily elevated temperature if the leading edge were maintained at 32° F. Such a distribution indicates poor utilization of the available heat.

SUMMARY OF RESULTS

With the use of standard production-model unpartitioned hollow steel propeller blades modified with shank and tip openings to permit internal passage of heated air for propeller icing protection, the following results were obtained for the conditions of icing to which the propeller was subjected:

1. Adequate ice protection was afforded with a heating rate of 40,000 Btu per hour per blade.

2. With a heating rate less than 40,000 Btu per hour per blade, icing protection failed because of significant ice accretions on the leading edge.

3. The chordwise distribution of heat was unsatisfactory with most of the available heat being dissipated well back of the leading edge on both the thrust and camber faces instead of at the leading edge where most needed.

4. A low utilization of available heat for icing protection was indicated by heat-exchanger effectiveness of approximately 47 percent.

Flight Propulsion Research Laboratory
National Advisory Committee for Aeronautics
Cleveland, Ohio, January 15, 1948.

REFERENCES

1. Lewis, James P.: An Investigation of De-Icing Effectiveness of External Electric Heaters for Propeller Blades. NACA TN No. 1520, 1948.

2. Darsow, John F., and Selna, James.: A Flight Investigation of the Thermal Performance of an Air-Heated Propeller. NACA TN No. 1178, 1947.

3. Carson, Blake W., Jr., and Maynard, Julian D.: Investigation of the Effect of Tip Modification and Thermal De-Icing Air Flow on Propeller Performance. NACA TN No. 1111, 1946.

4. Gray, V. H., and Campbell, R. G.: A Method For Estimating Heat Requirements for Ice Prevention on Gas-Heated Hollow Propeller Blades. NACA TN No. 1494, 1947.

5. Carson, Blake W., Jr., and Maynard, Julian D.: The Effect of Simulated Icing on Propeller Performance. NACA TN No. 1084, 1946.

Page intentionally left blank

Page intentionally left blank

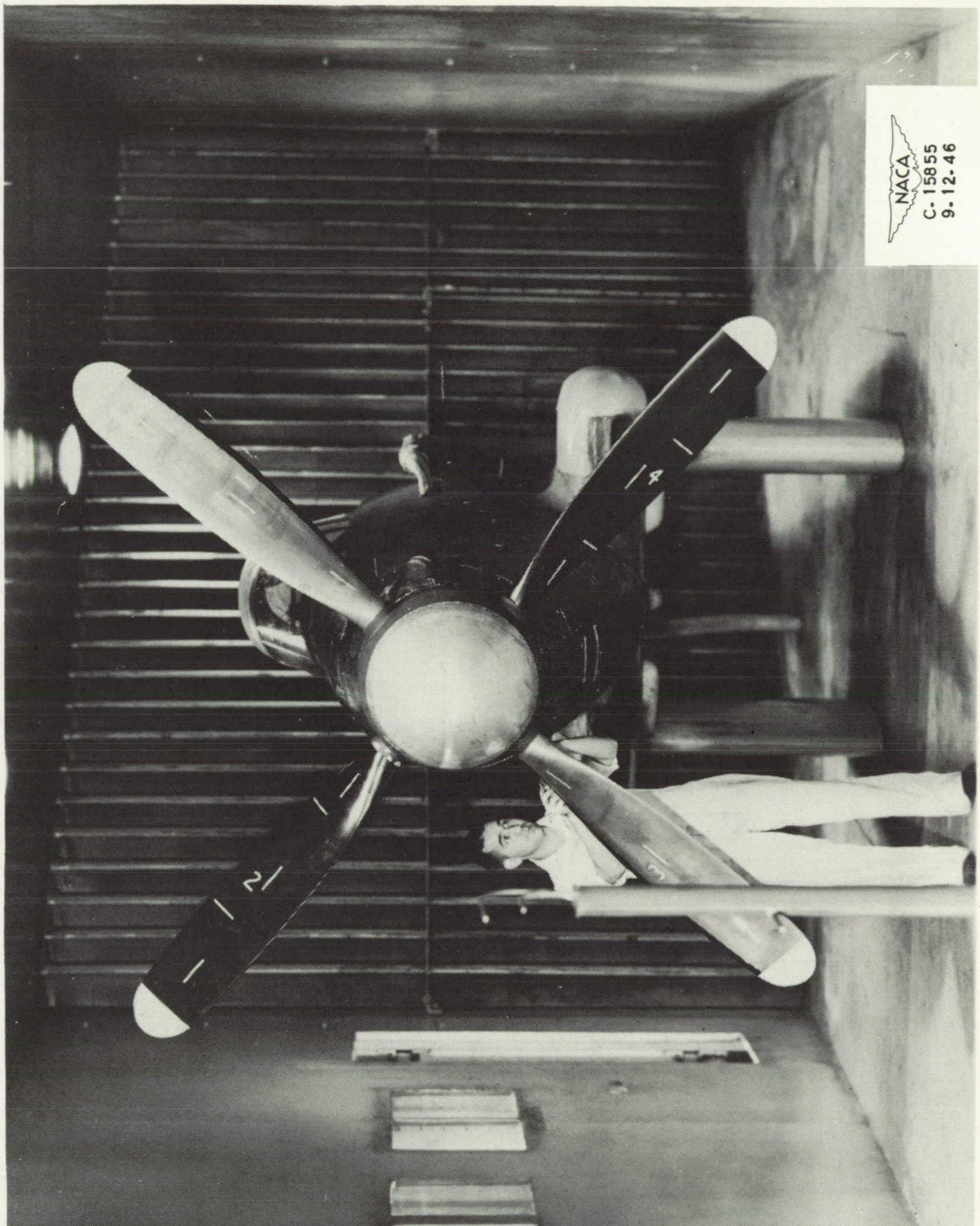

Figure 1. - Tunnel installation of hollow steel air-heated propeller for icing investigation.

Page intentionally left blank

Page intentionally left blank

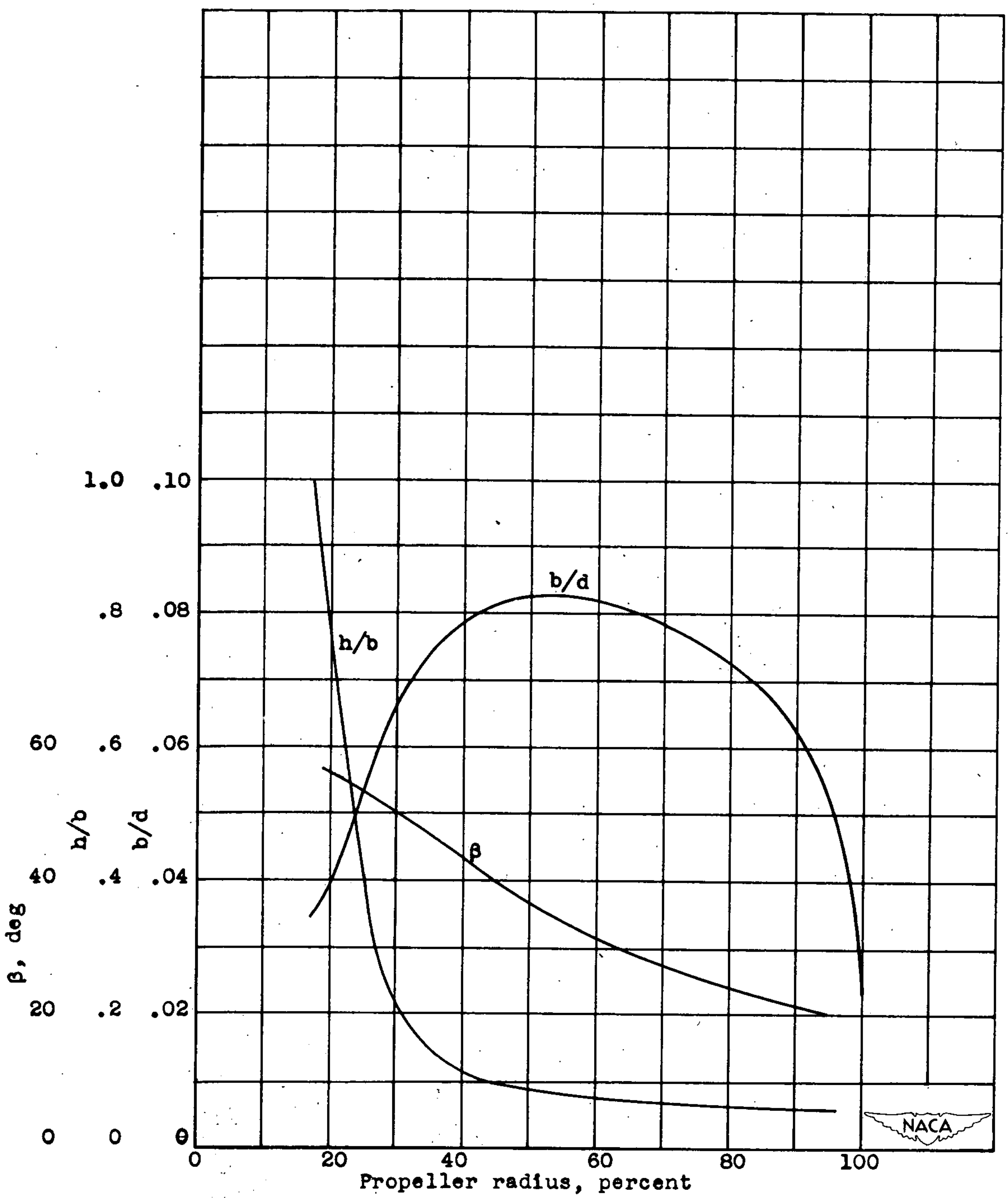

Figure 2.- Blade characteristics of hollow steel air-heated propeller. Propeller diameter, 10 feet, 2 inches; β, blade angle, degrees; h, blade thickness, feet; b, blade chord, feet; d, propeller diameter, feet.

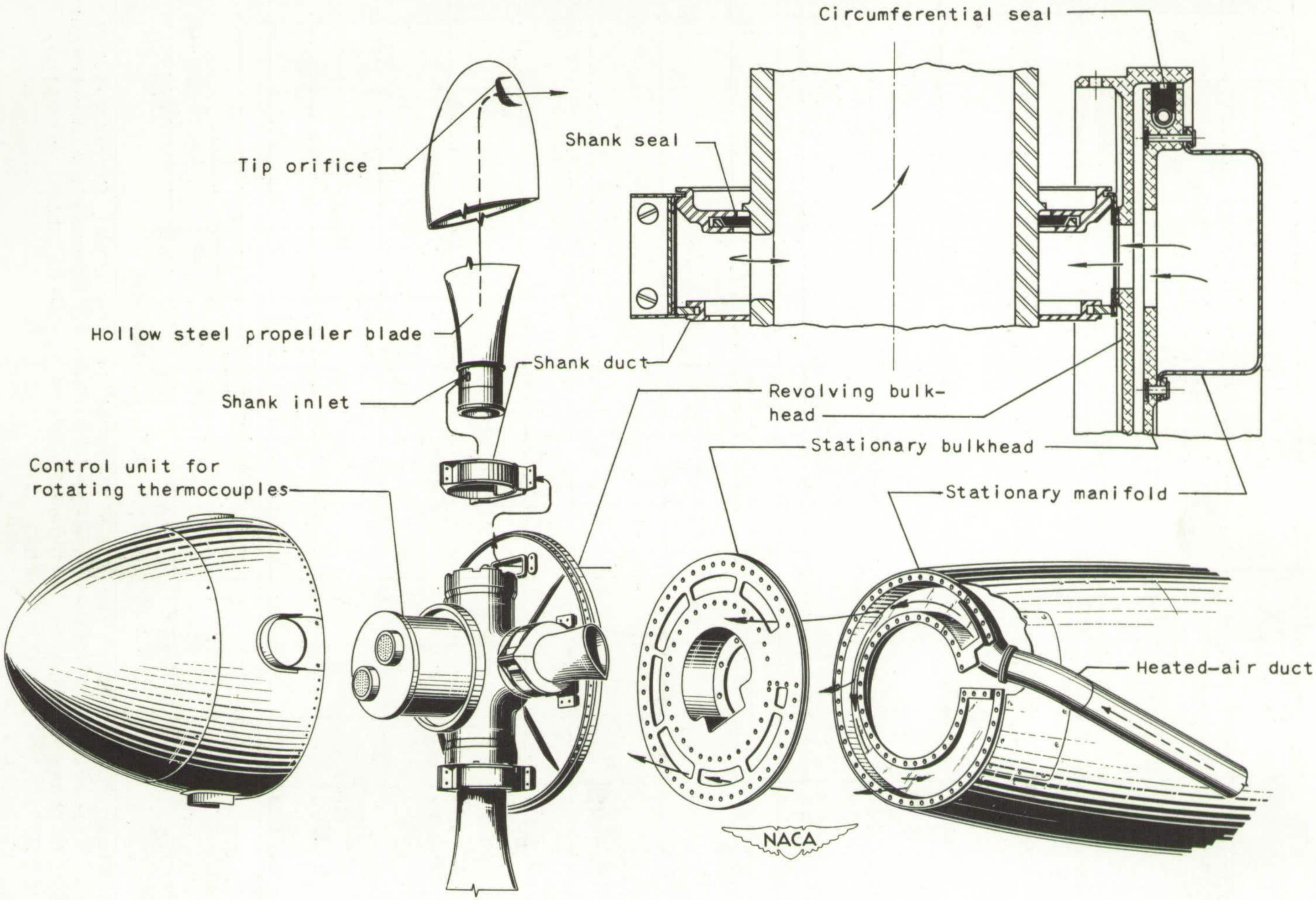

Figure 3. - Details of air-heated propeller installation.

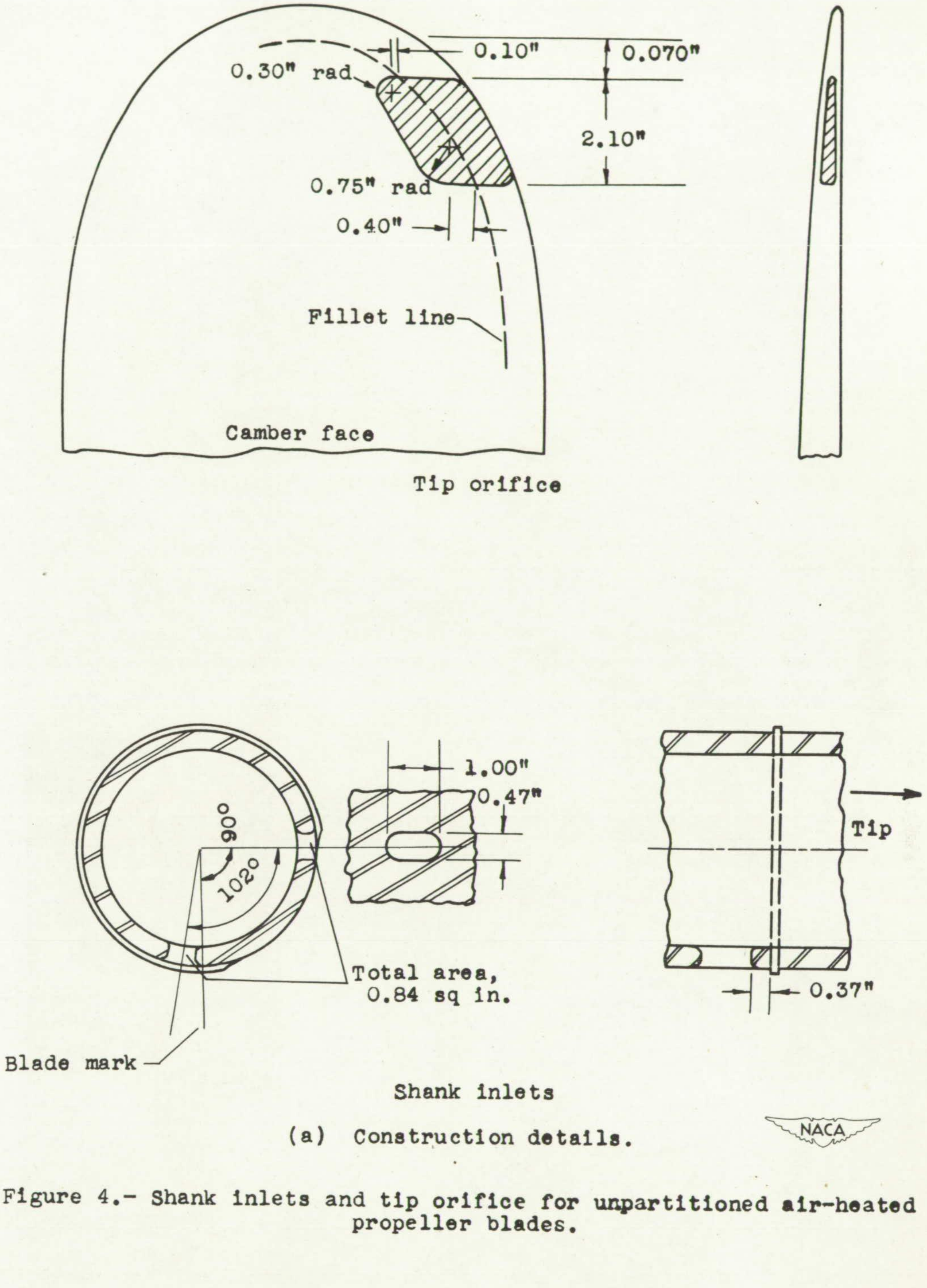

(a) Construction details.

Figure 4.- Shank inlets and tip orifice for unpartitioned air-heated propeller blades.

Page intentionally left blank

Page intentionally left blank

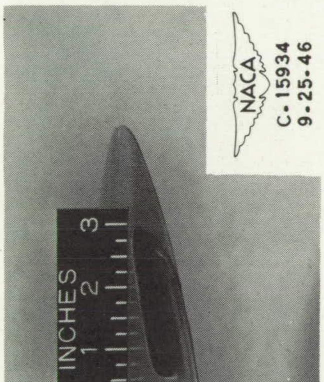

C-15934
9-25-46

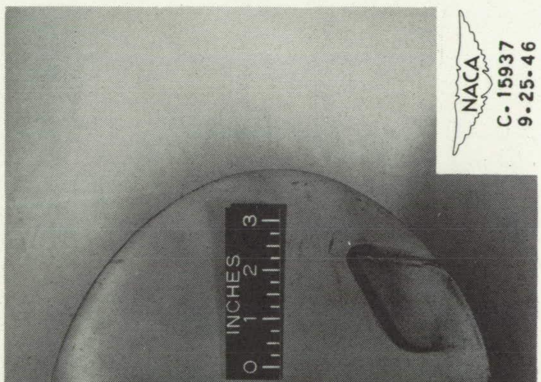

C-15937
9-25-46

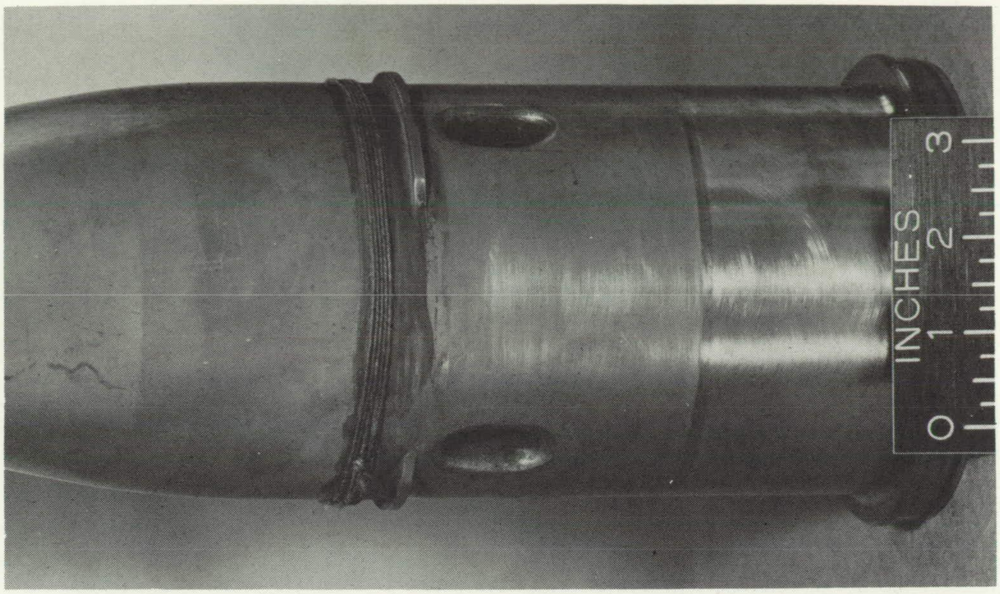

C-15938
9-25-46

(b) Photographs of tip and shank openings in blade.

Figure 4. - Concluded. Shank inlets and tip orifice for unpartitioned air-heated propeller blades.

Page intentionally left blank

Page intentionally left blank

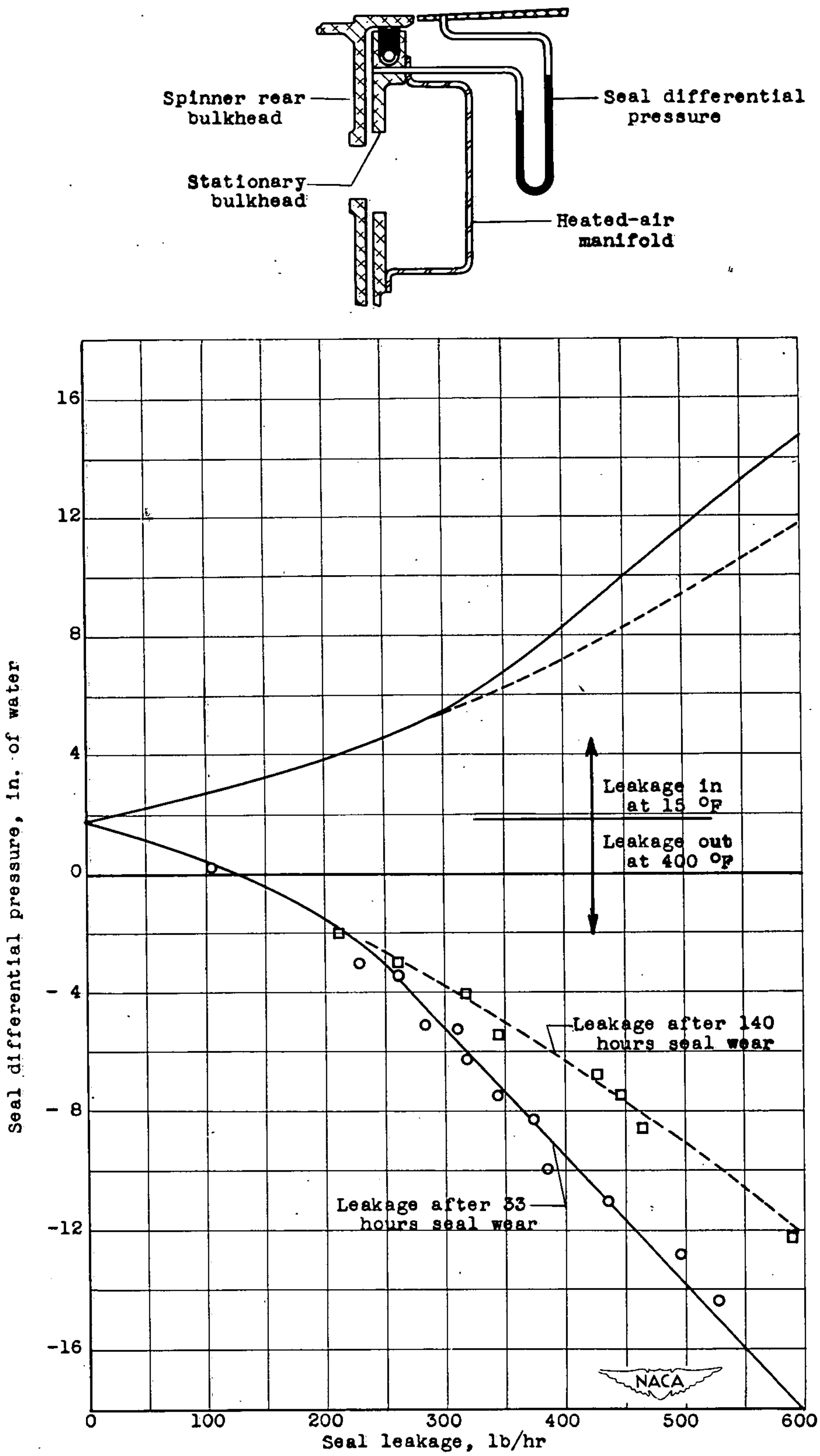

Figure 5. - Calibration of air leakage past spinner circumferential seal and shank seals with blade inlets closed.

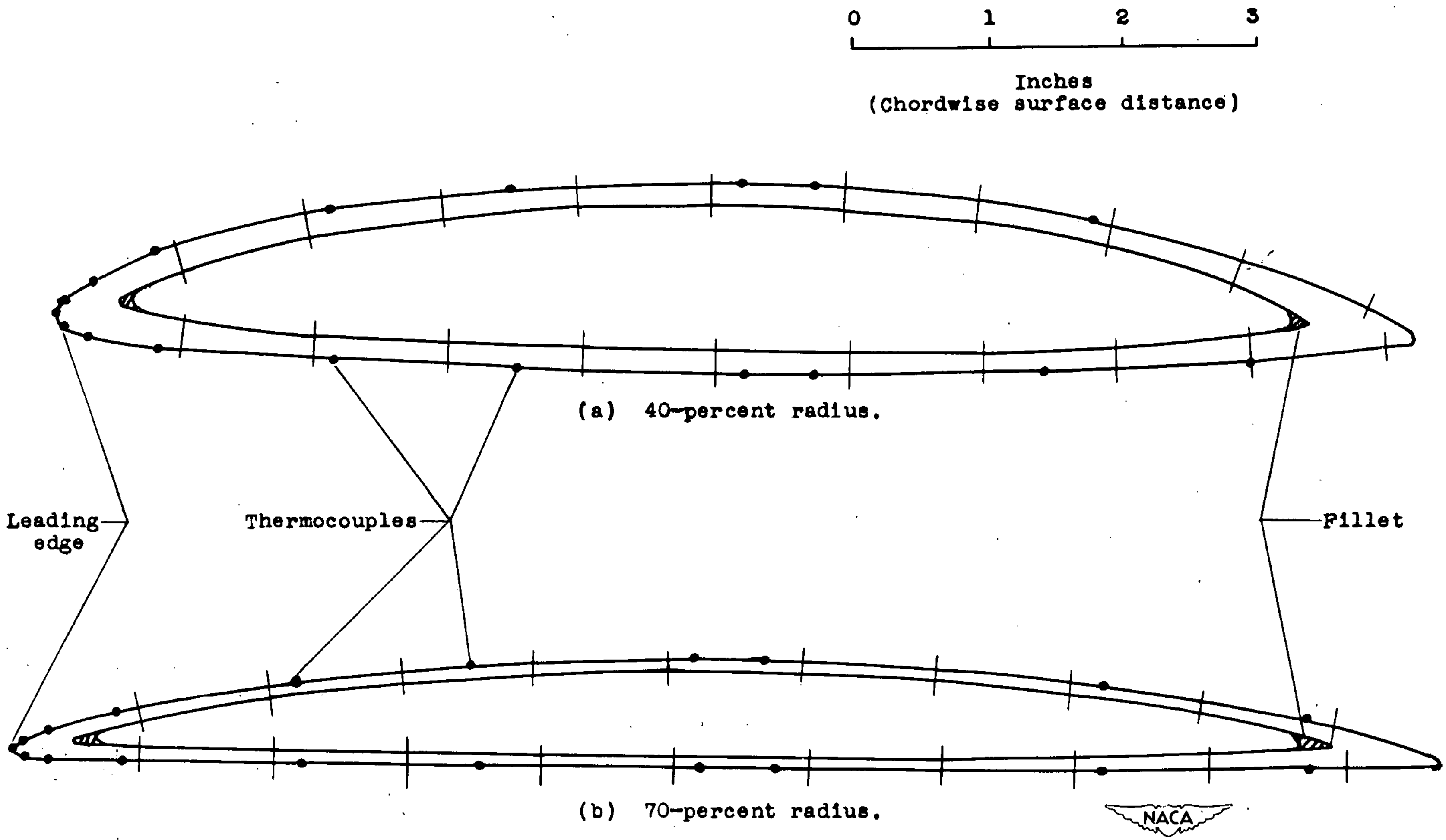

Figure 6.- Chordwise thermocouple locations.

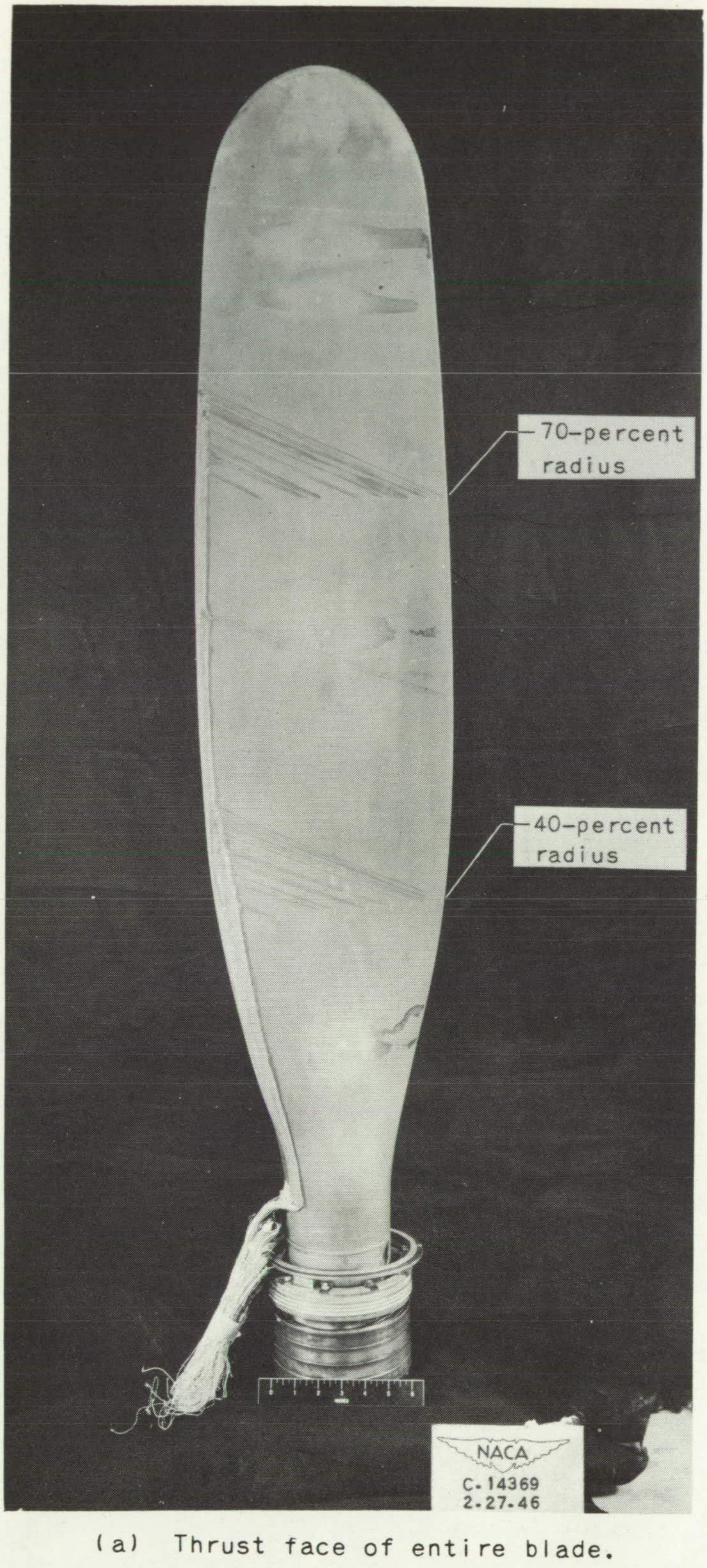

(a) Thrust face of entire blade.

Figure 7. - Blade-surface thermocouple installation before application of final protective coating.

Page intentionally left blank

Page intentionally left blank

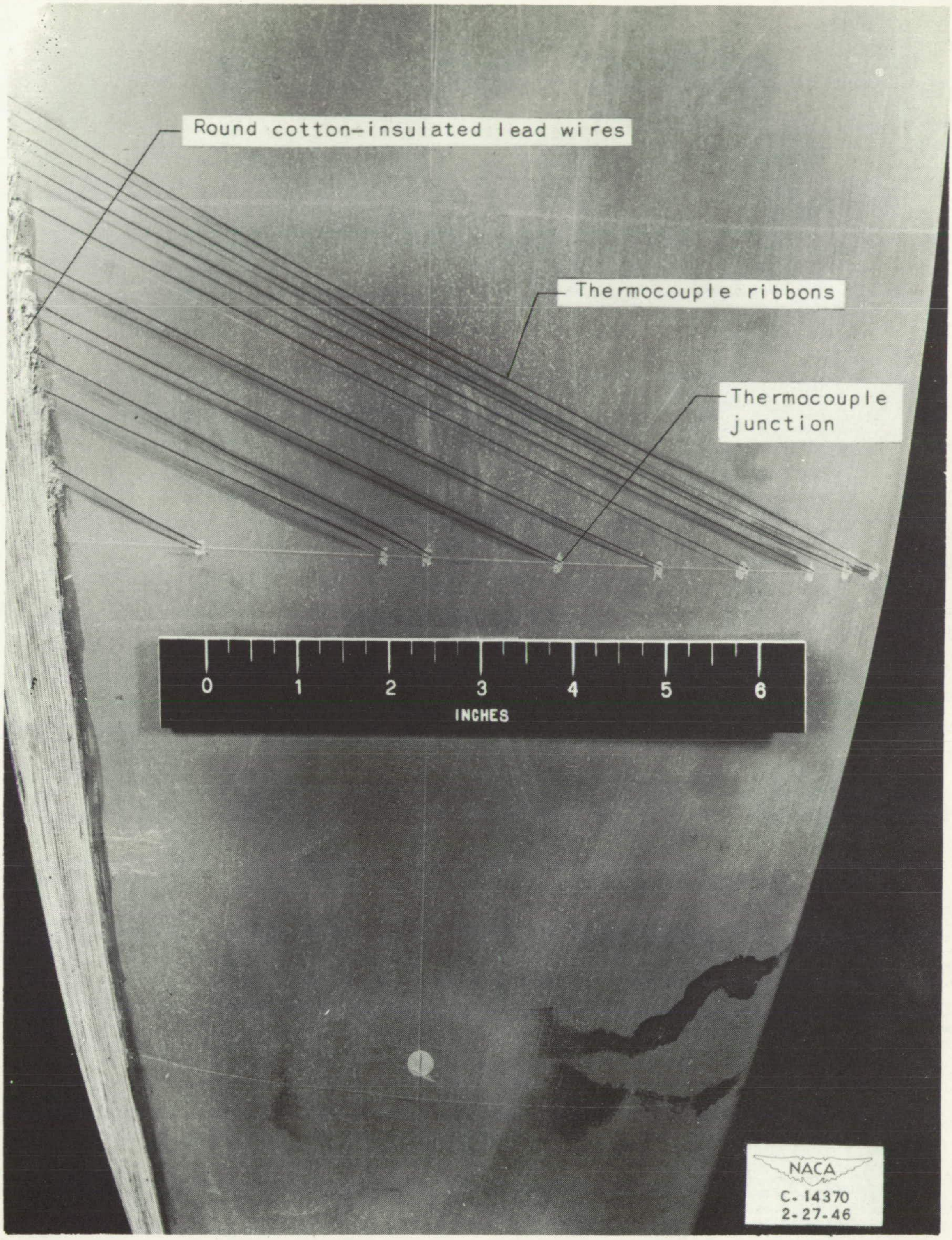

(b) 40-percent radius station.

Figure 7. - Concluded. Blade-surface thermocouple installation before application of final protective coating.

Page intentionally left blank

Page intentionally left blank

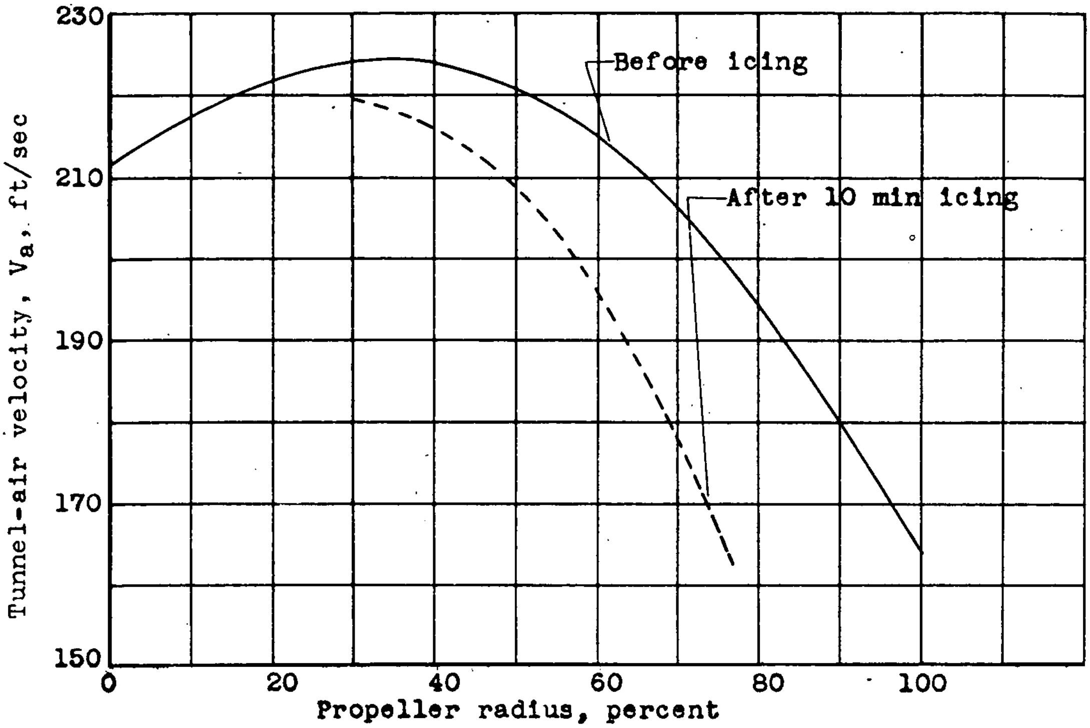

Figure 8.- Radial distribution of tunnel-air velocity at propeller plane before and after 10 minutes icing. Propeller not operating.

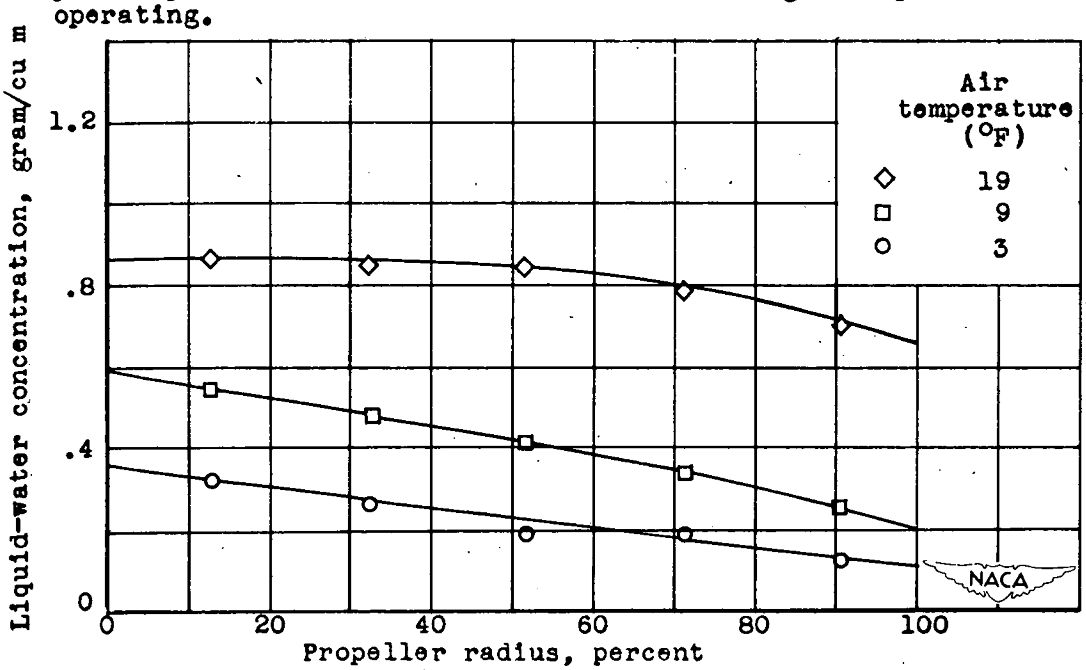

Figure 9.- Radial distribution of liquid-water concentration at propeller plane during icing.

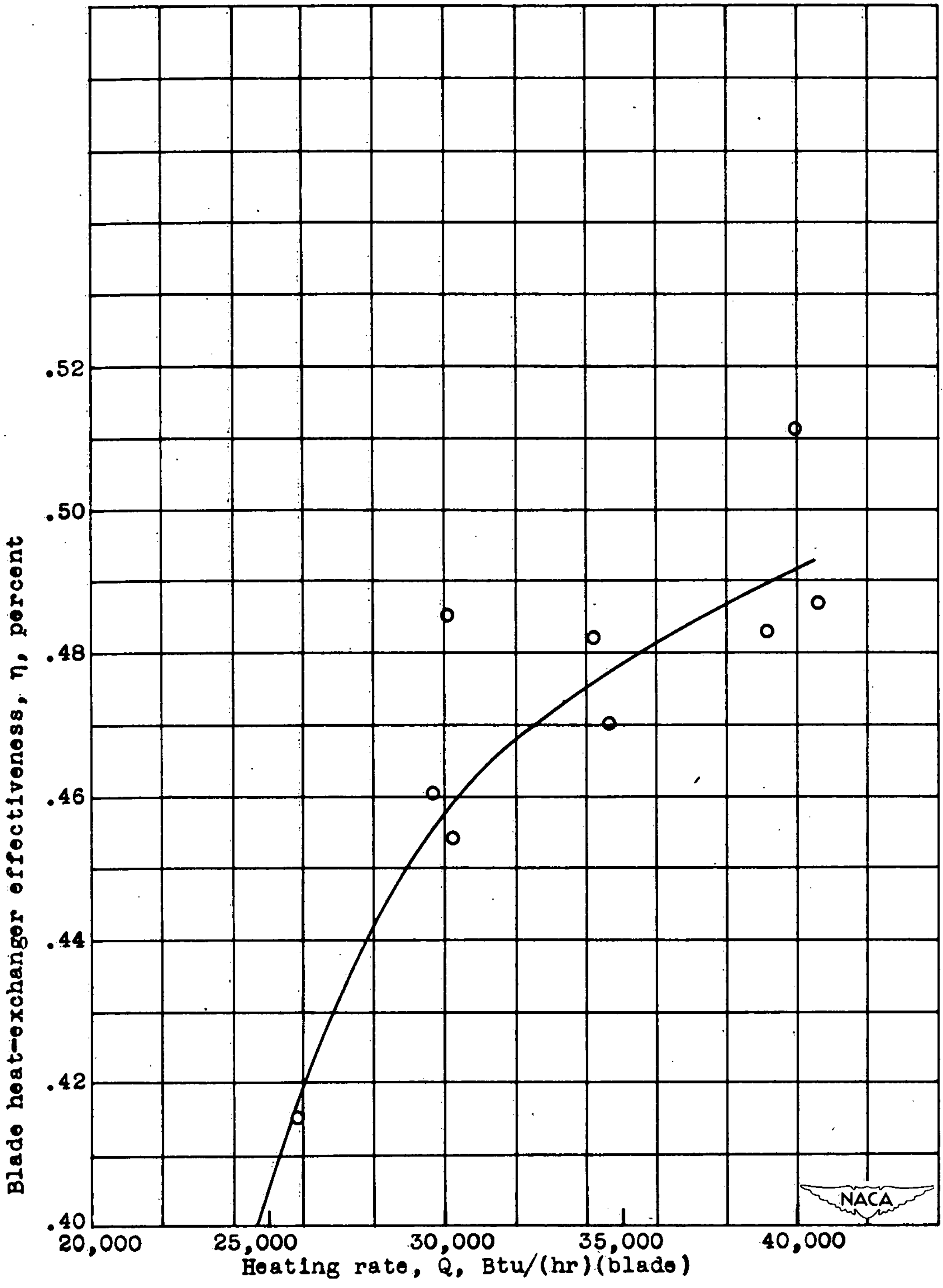

Figure 10.- Heat-exchanger effectiveness of heated-air propeller blade. No sprays; propeller speed, 1050 rpm; blade angle, 28°; blade air flow, 420 pounds per hour; tunnel-air temperature, 5° to 15° F.

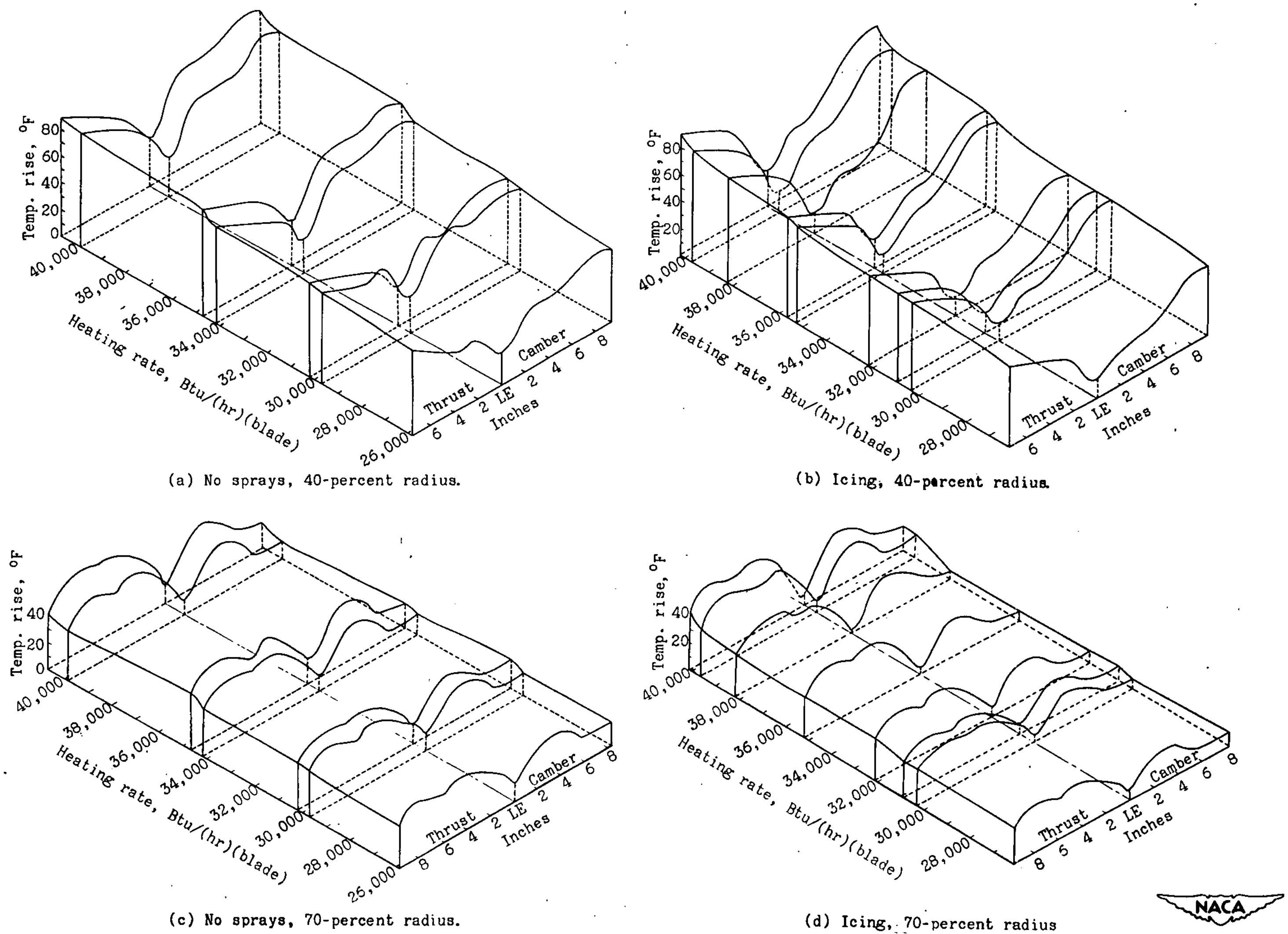

Figure 11. - Chordwise distribution of blade-surface temperature rise as function of heating rate to blade. Propeller speed, 1050 rpm; blade angle, 28°.

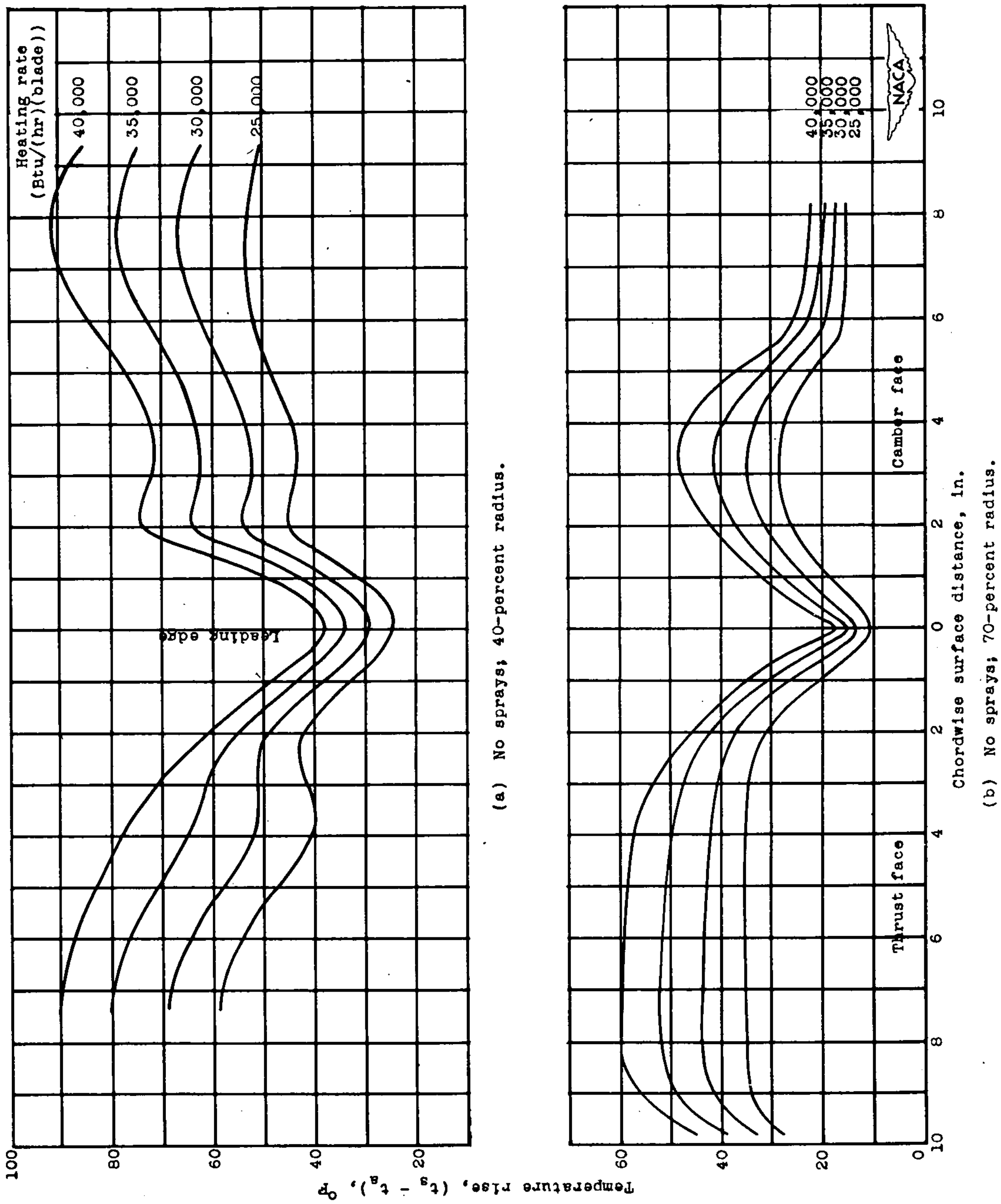

Figure 12. - Effect of increasing heating rate on propeller-blade-surface temperature rise. Propeller speed, 1050 rpm; blade angle, 28°.

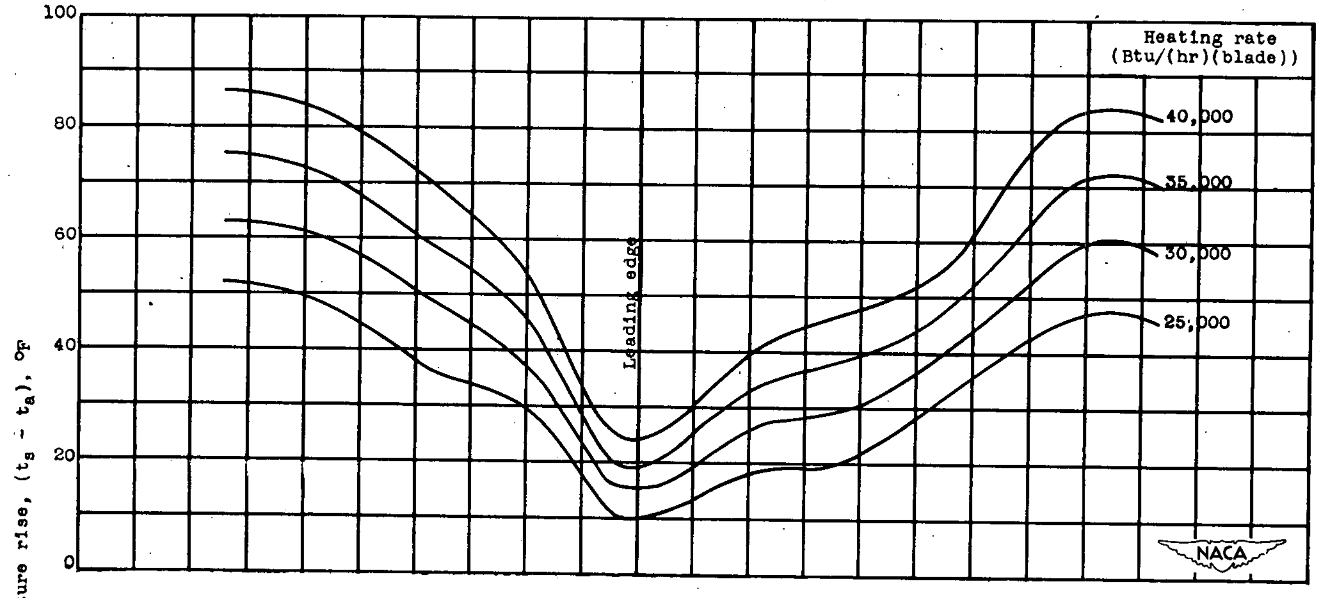

(c) Icing conditions, 40-percent radius.

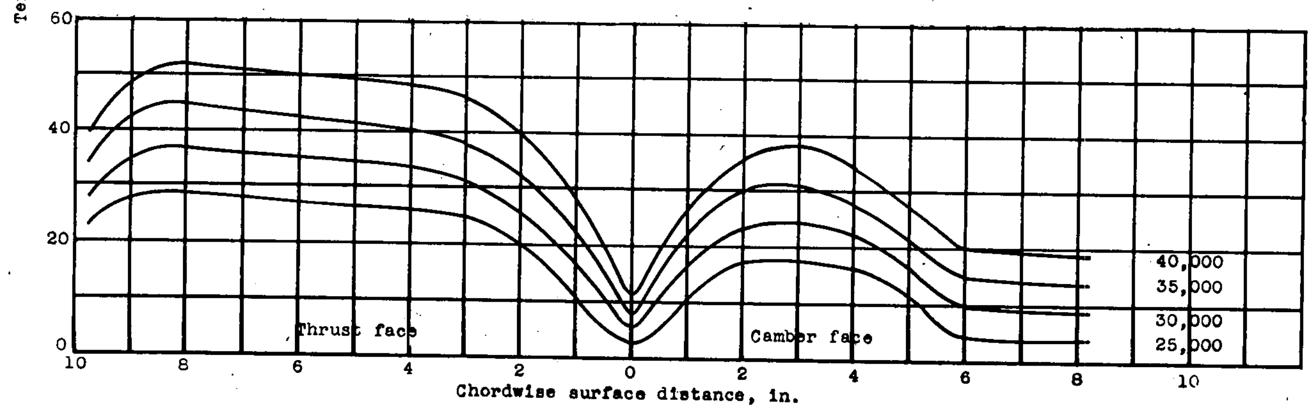

(d) Icing conditions, 70-percent radius.

Figure 12.- Concluded. Effect of increasing heating rate on propeller-blade-surface temperature rise. Propeller speed, 1050 rpm; blade angle, 28°.

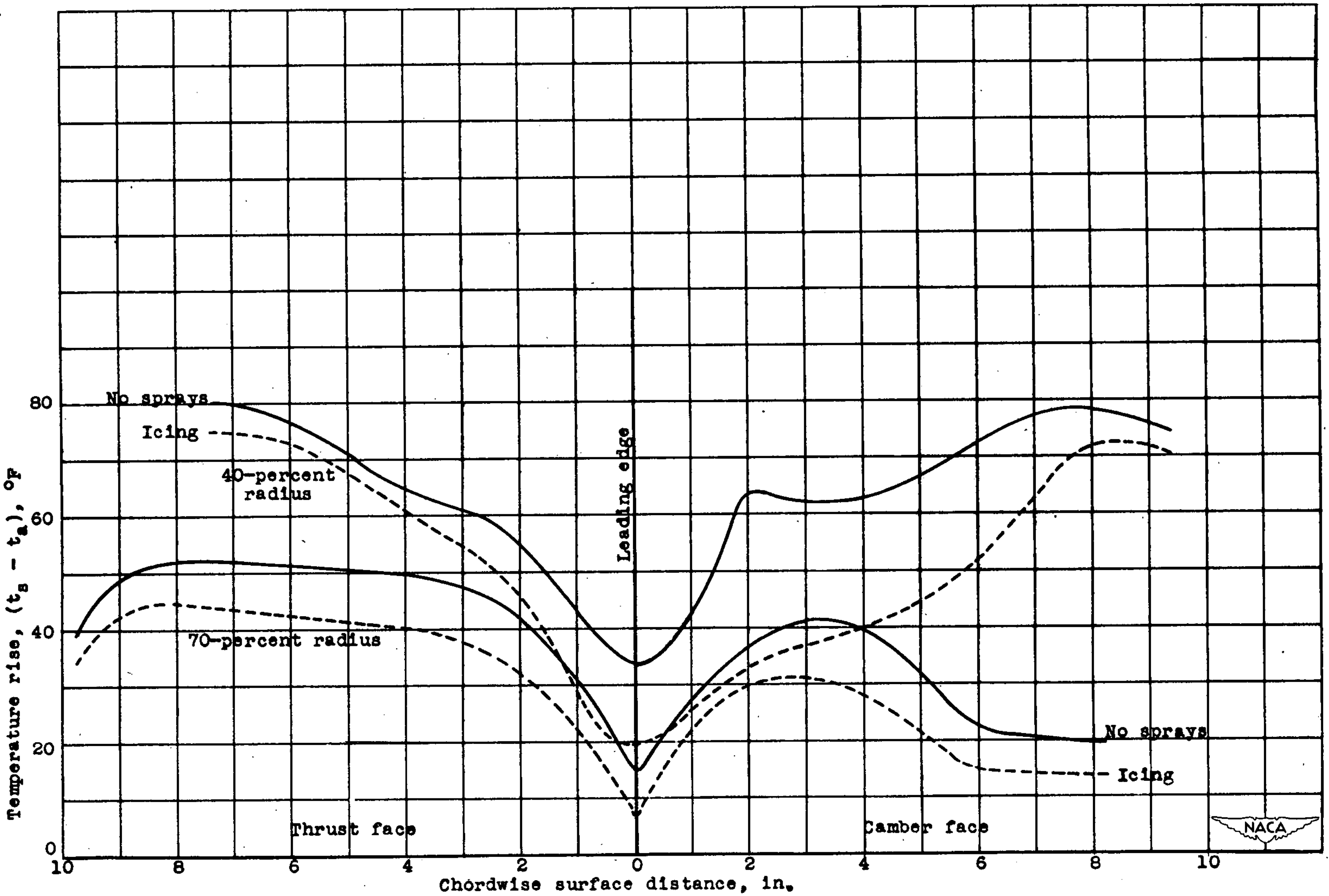

Figure 13.- Comparison of blade-surface temperature rise above tunnel-air temperature for no-spray and icing conditions at 40- and 70-percent blade radius. Blade angle, 28°; propeller speed, 1050 rpm; heating rate, 35,000 Btu per hour per blade.

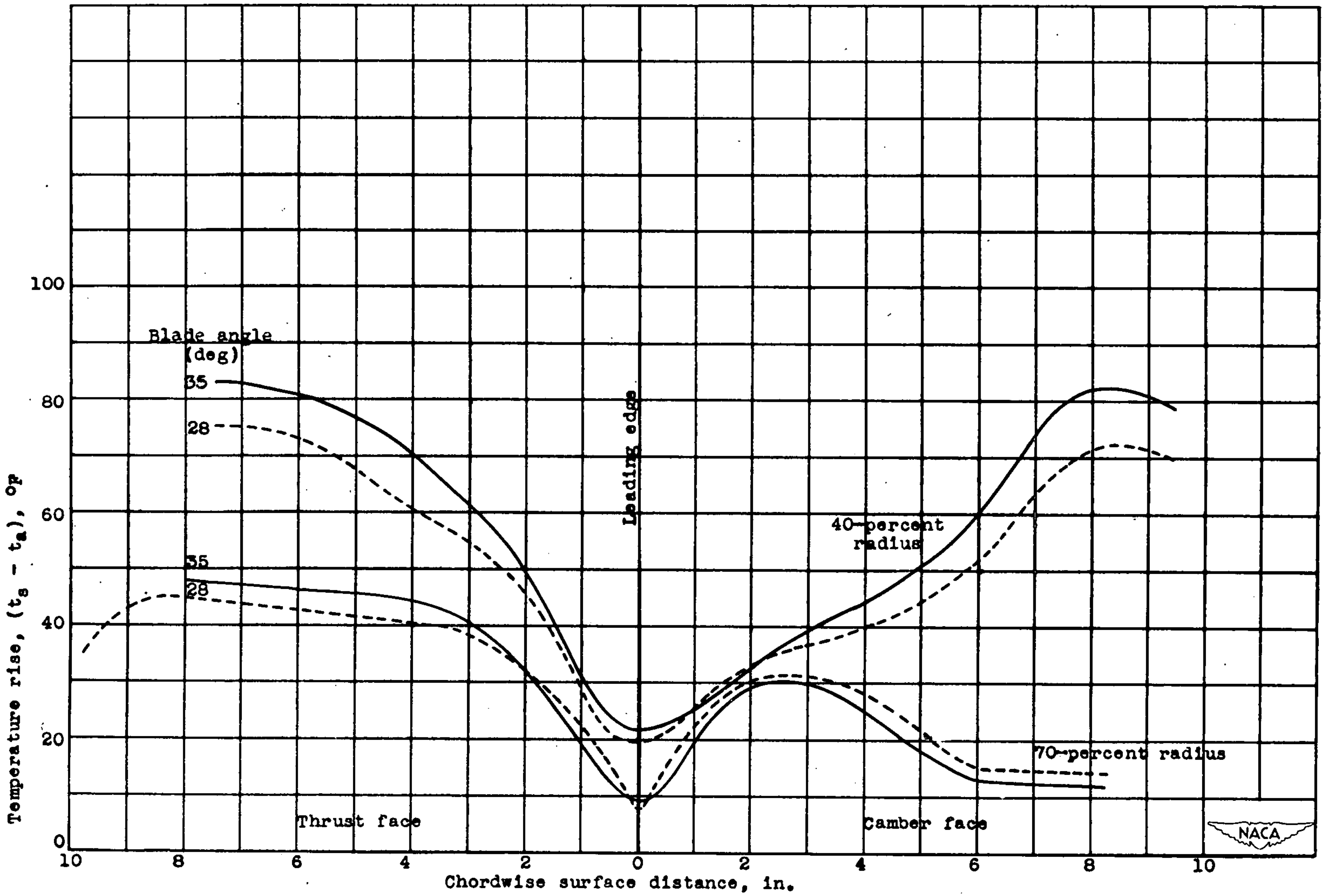

Figure 14.- Comparison of blade-surface temperature rise above tunnel-air temperature for icing conditions at 40- and 70-percent blade radius, using blade angles of 28° to 35° with propeller speeds of 1050 and 850 rpm, respectively. Heating rate, 35,000 Btu per hour per blade.

Page intentionally left blank

Page intentionally left blank

Camber face, blade 4

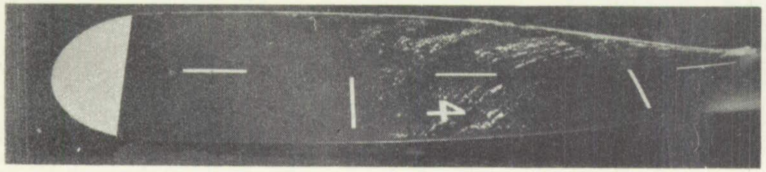

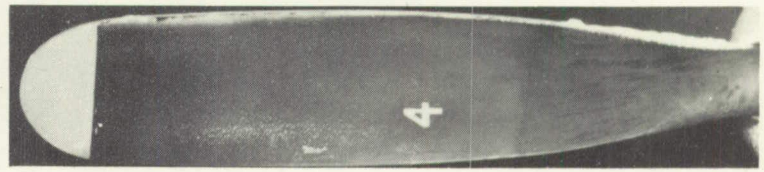

Thrust face, blade 4

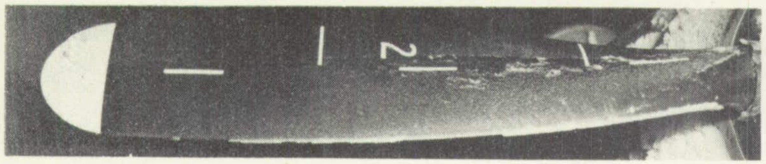

Camber face, blade 2

Camber face, blade 3

C-20349
1.7.48

(a) Tunnel-air temperature, 16° F.

(b) Tunnel-air temperature, 10° F.

Figure 15. - Typical ice formations on unneated propeller blades and airplane fuselage after 10-minute icing period. Blade angle, 28°; propeller speed, 1050 rpm.

Page intentionally left blank

Page intentionally left blank

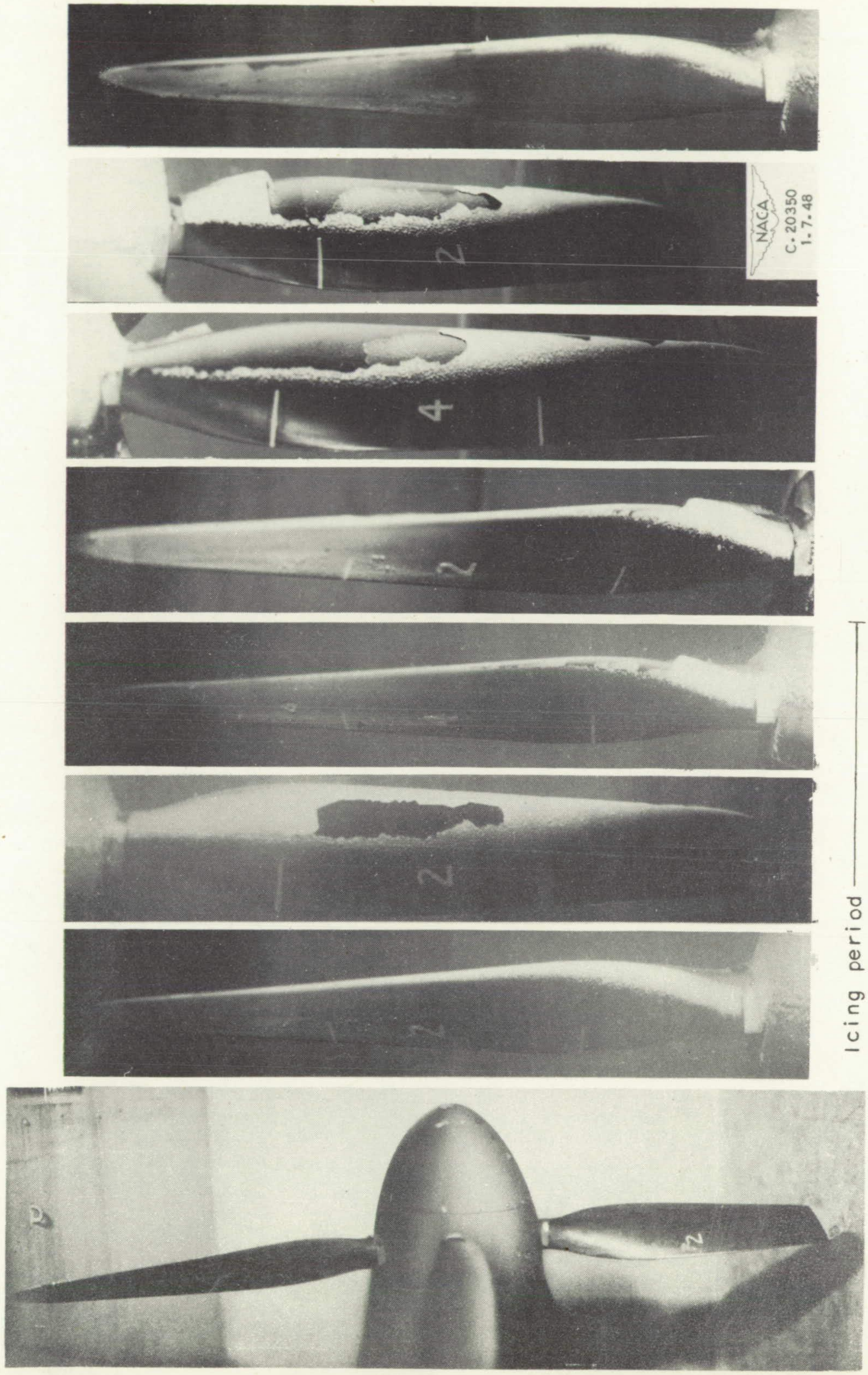

Figure 16. - Stroboscopic photographs of unheated propeller blades during and following 10-minute icing period. Tunnel-air temperature, 11° F; blade angle, 35°; propeller speed, 850 rpm.

Page intentionally left blank

Page intentionally left blank

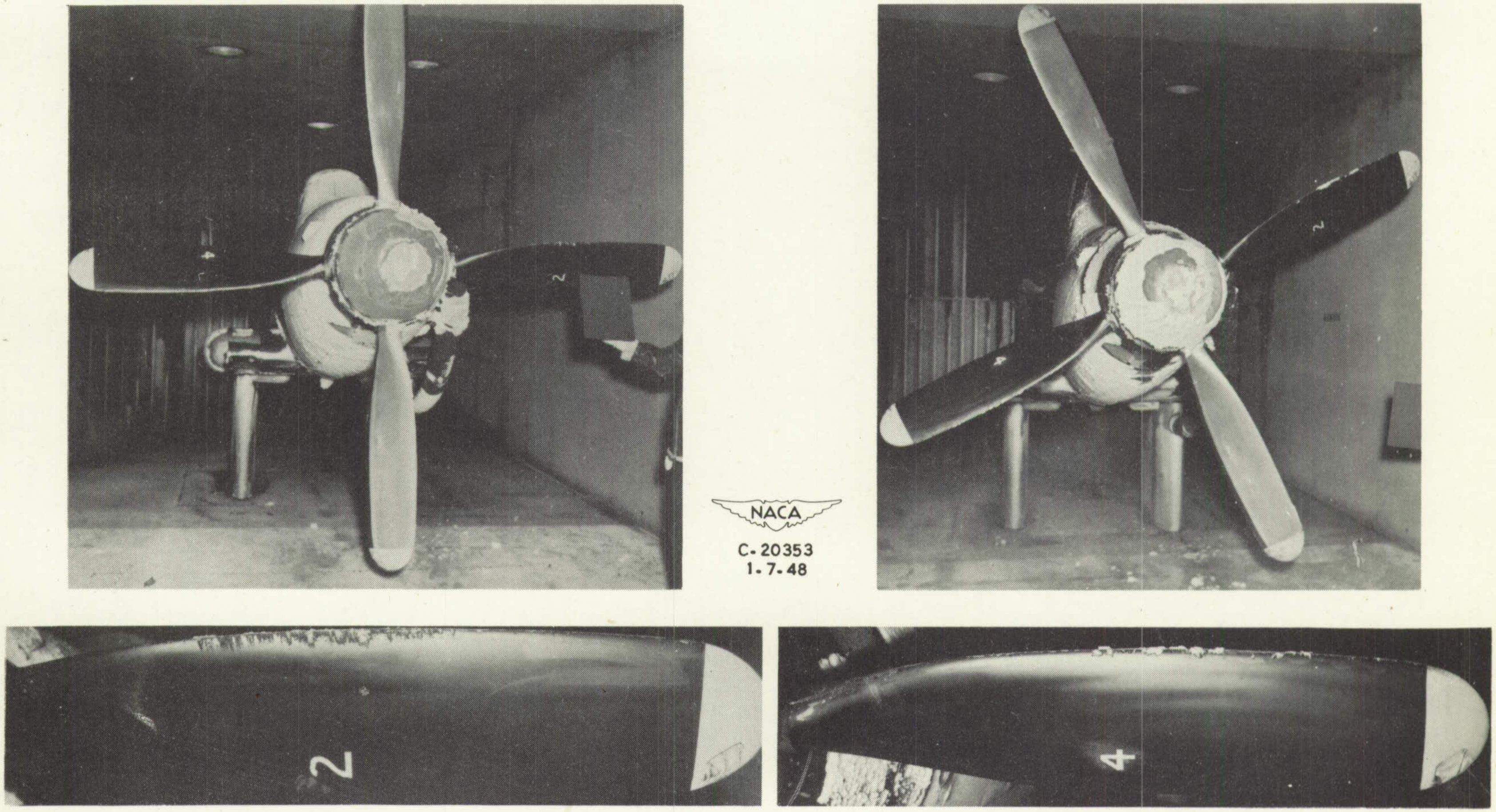

(a) Heating rate, 31,000 Btu per hour per blade; tunnel-air temperature, 17° F.

(b) Heating rate, 37,400 Btu per hour per blade; tunnel-air temperature, 17° F.

Figure 17.- Residual ice formations on camber face of propeller blades after 10-minute icing period. Blade angle, 28°; propeller speed, 1050 rpm.

Page intentionally left blank

Page intentionally left blank

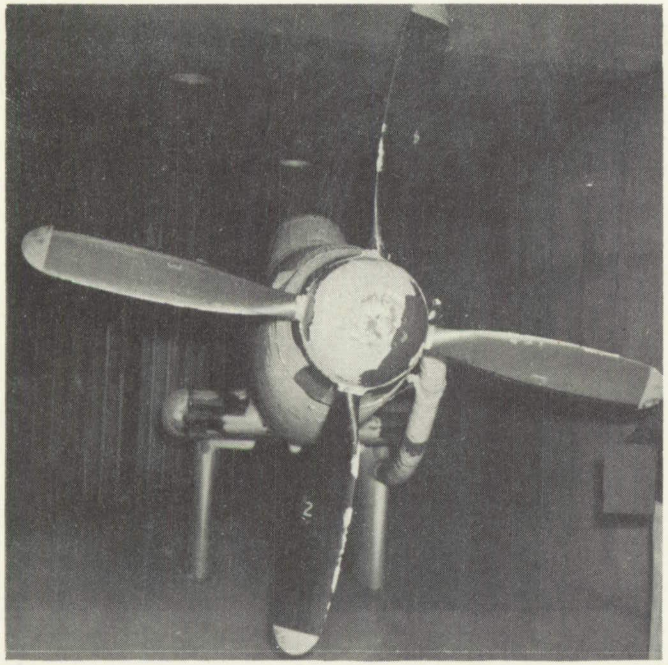

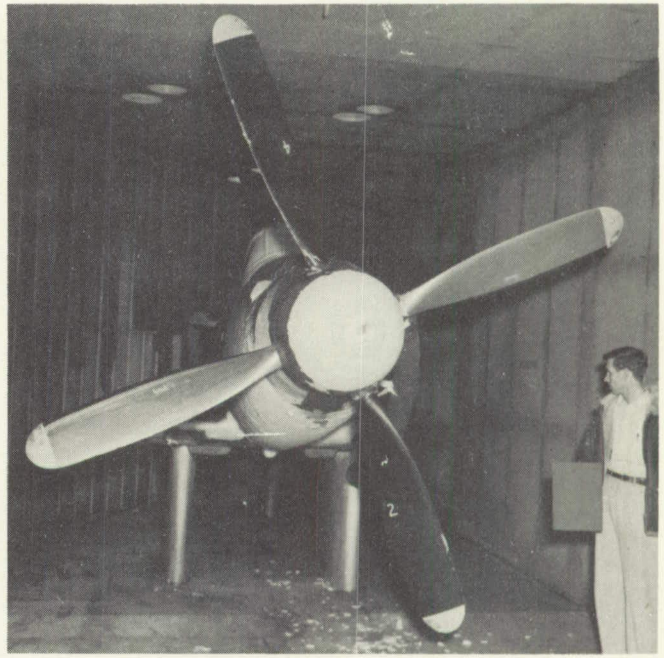

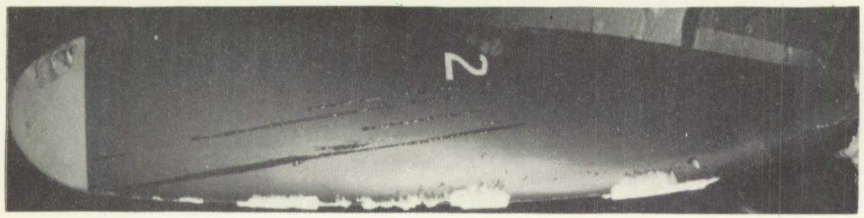

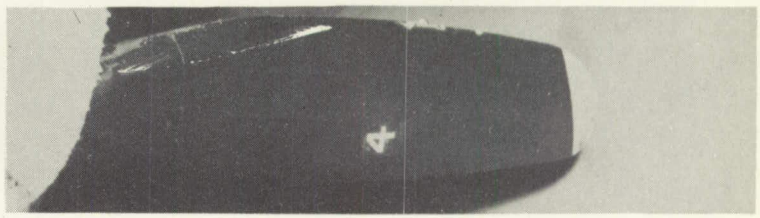

NACA
C-20354
1.7.48

(c) Heating rate, 26,000 Btu per hour per blade; tunnel-air temperature, 10° F.

(d) Heating rate, 39,400 Btu per hour per blade; tunnel-air temperature, 10° F.

Figure 17. - Continued. Residual ice formations on camber face of propeller blades after 10-minute icing period. Blade angle, 28°; propeller speed, 1050 rpm.

Page intentionally left blank

Page intentionally left blank

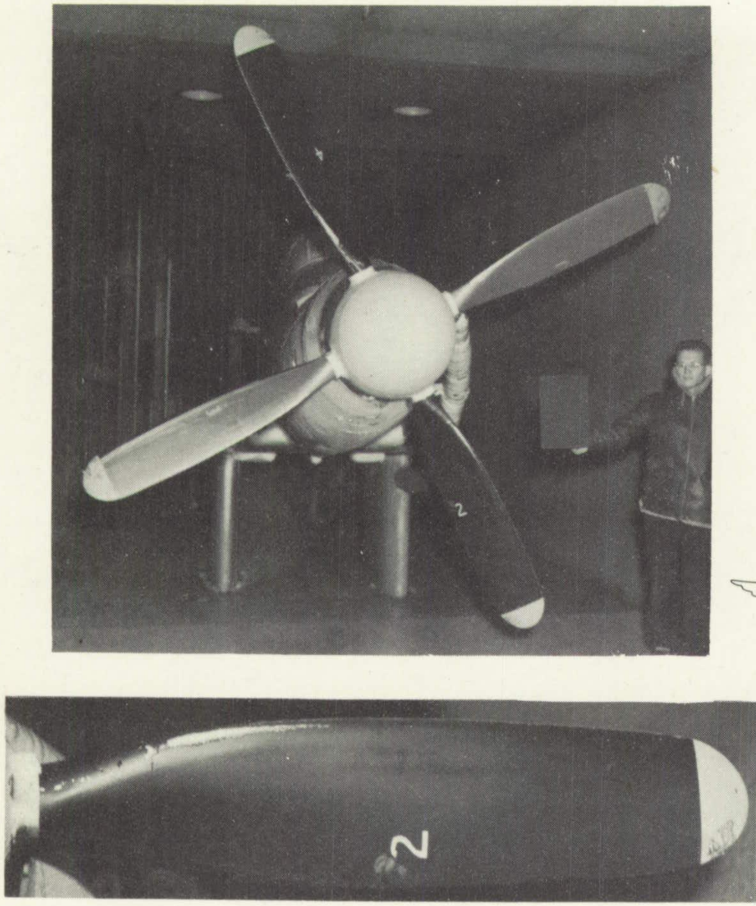

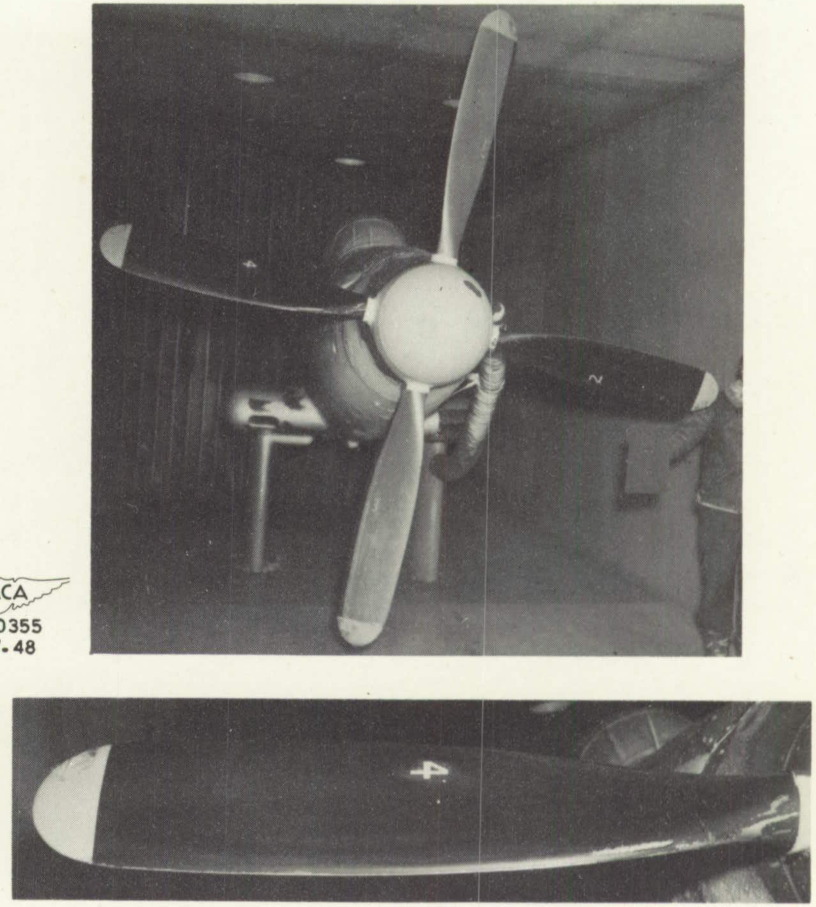

NACA
C-20355
1.7.48

(e) Heating rate, 31,900 Btu per hour per blade; tunnel-air temperature, -2° F.

(f) Heating rate, 40,000 Btu per hour per blade; tunnel-air temperature, -2° F.

Figure 17. - Concluded. Residual ice formations on camber face of propeller blades after 10-minute icing period. Blade angle, 28°; propeller speed, 1050 rpm.

Page intentionally left blank

Page intentionally left blank

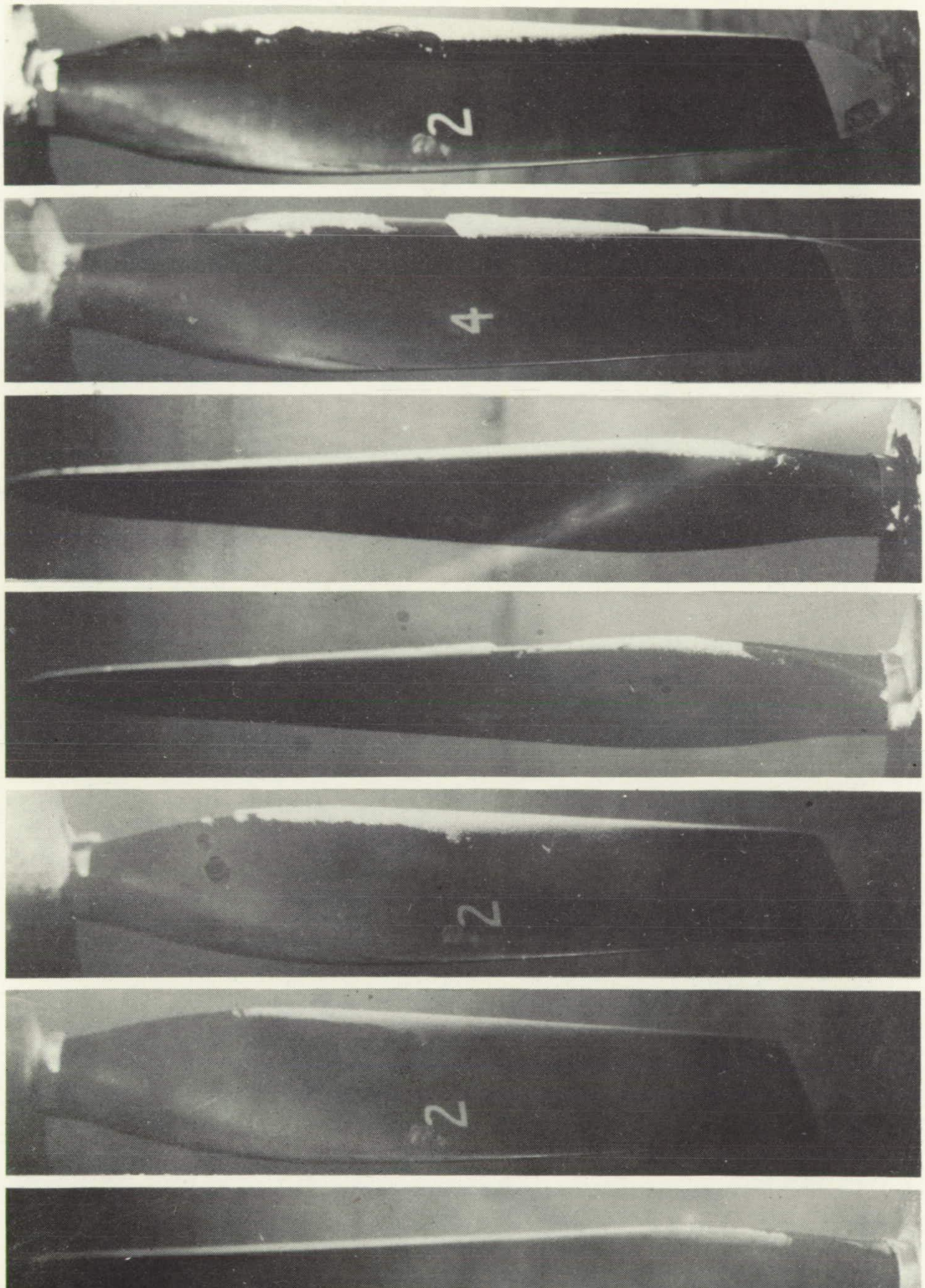

(a) Heating rate, 30,800 Btu per hour per blade; tunnel-air temperature, 9° F.

Figure 18. - Stroboscopic photographs of air-heated propeller blades during and following 10-minute icing period. Blade angle, 35°; propeller speed, 850 rpm.

Page intentionally left blank

Page intentionally left blank

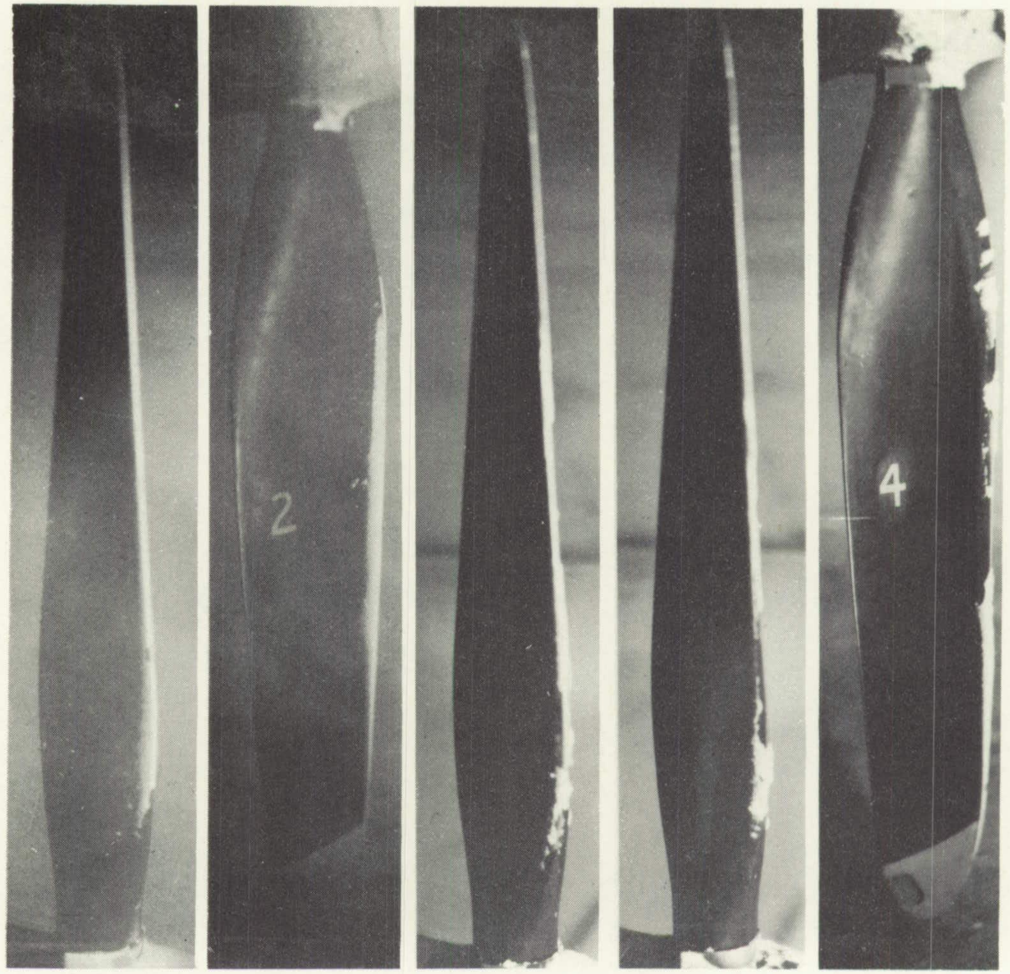

Icing period
10:40 2:10 10:40 11:30 12:20
Time, min:sec

NACA
C-20352
1-7-48

(b) Heating rate, 34,400 Btu per hour per blade; tunnel-air temperature, 11° F.

Figure 18. - Concluded. Stroboscopic photographs of air-heated propeller blades during and following 10-minute icing period. Blade angle, 35°; propeller speed, 850 rpm.